Facies (2010) 56:59–87
DOI 10.1007/s10347-009-0190-8

ORIGINAL ARTICLE

Facies analysis of a large-scale Jurassic shelf-lagoon: the Kamar-e-Mehdi Formation of east-central Iran

Markus Wilmsen · Franz T. Fürsich · Kazem Seyed-Emami · Mahmoud R. Majidifard · Massoud Zamani-Pedram

Received: 20 November 2008 / Accepted: 20 April 2009 / Published online: 15 May 2009

Abstract The Callovian–Lower Kimmeridgian Kamar-e-Mehdi Formation of the Tabas Block (east-central Iran) is an up to 1,350-m-thick, fine-grained, marly-calcareous unit containing a basal Echellon Limestone Member (up to 180 m thick) and a terminal Nar Limestone Member (up to 100 m thick). The formation was deposited in a relatively deep shelf-lagoon that was part of the large-scale carbonate system of the Esfandiar Subgroup, extending N–S for about 500 km along the strike with a width of up to 100 km. The lagoonal Kamar-e-Mehdi Formation shows sedimentation rates of 150 m/myr, twice as high as those of the shelf-edge carbonate barrier (Esfandiar Platform). The repetitive lithologies and uniform depositional environment suggest equilibrium conditions between sedimentation and subsidence, related to constant slow rotation of the Tabas fault-block around a horizontal axis, the platform sitting on the crest, and the lagoon occupying the dip-slope. Lagoonal sedimentation was dominated by suspended carbonate mud and peloids from the eastern Esfandiar Platform whereas the subordinate siliciclastic material was derived from the west (Yazd Block). The diverse macrobenthos (mainly bivalves) suggests fully marine conditions for the major part of the Kamar-e-Mehdi Formation. However, towards the upper part, biotic impoverishment and the deposition of skeletal-poor, evaporitic sediments indicate increasing restriction. The overlying Magu Gypsum Formation marks the end of an arid basin-fill cycle and possibly forms an effective seal for hydrocarbon reservoirs in that area. The Esfandiar Subgroup was a Neotethys-facing carbonate margin, forming part of a belt of carbonate systems tracking the margins of the Iran Plate during Callovian to Late Jurassic times.

Keywords Callovian–Kimmeridgian · Esfandiar Subgroup · Shelf-lagoon · Micro- and biofacies · Palaeogeography

M. Wilmsen (✉)
Senckenberg Naturhistorische Sammlungen Dresden, Museum für Mineralogie und Geologie, Sektion Paläozoologie, Königsbrücker Landstrasse 159, 01109 Dresden, Germany
e-mail: markus.wilmsen@senckenberg.de

F. T. Fürsich
GeoZentrum Nordbayern, Fachgruppe PaläoUmwelt, Friedrich-Alexander-Universität Erlangen-Nürnberg, Loewenichstr. 28, 91054 Erlangen, Germany

K. Seyed-Emami
School of Mining Engineering, University College of Engineering, University of Tehran, PO Box 11365-4563, Tehran, Iran

M. R. Majidifard · M. Zamani-Pedram
Geological Survey of Iran, PO Box 131851-1494, Tehran, Iran

Introduction

Jurassic rocks are widely distributed and superbly exposed in the Tabas area of east-central Iran (Fig. 1). The Lower and large parts of the Middle Jurassic are characterized by siliciclastic sequences, whereas the Callovian to Upper Jurassic rocks show a predominance of carbonate sediments which were lithostratigraphically included into the Esfandiar Subgroup by Wilmsen et al. (2003). The Esfandiar Subgroup represents a low-latitude carbonate system, the basinal, slope and platform sediments of which were described in detail by Schairer et al. (2000, 2003) and Fürsich et al. (2003a). The objective of this study is the stratigraphical and facies analysis of the large-scale shelf-lagoon represented by the Kamar-e-Mehdi Formation, part of the carbonate system

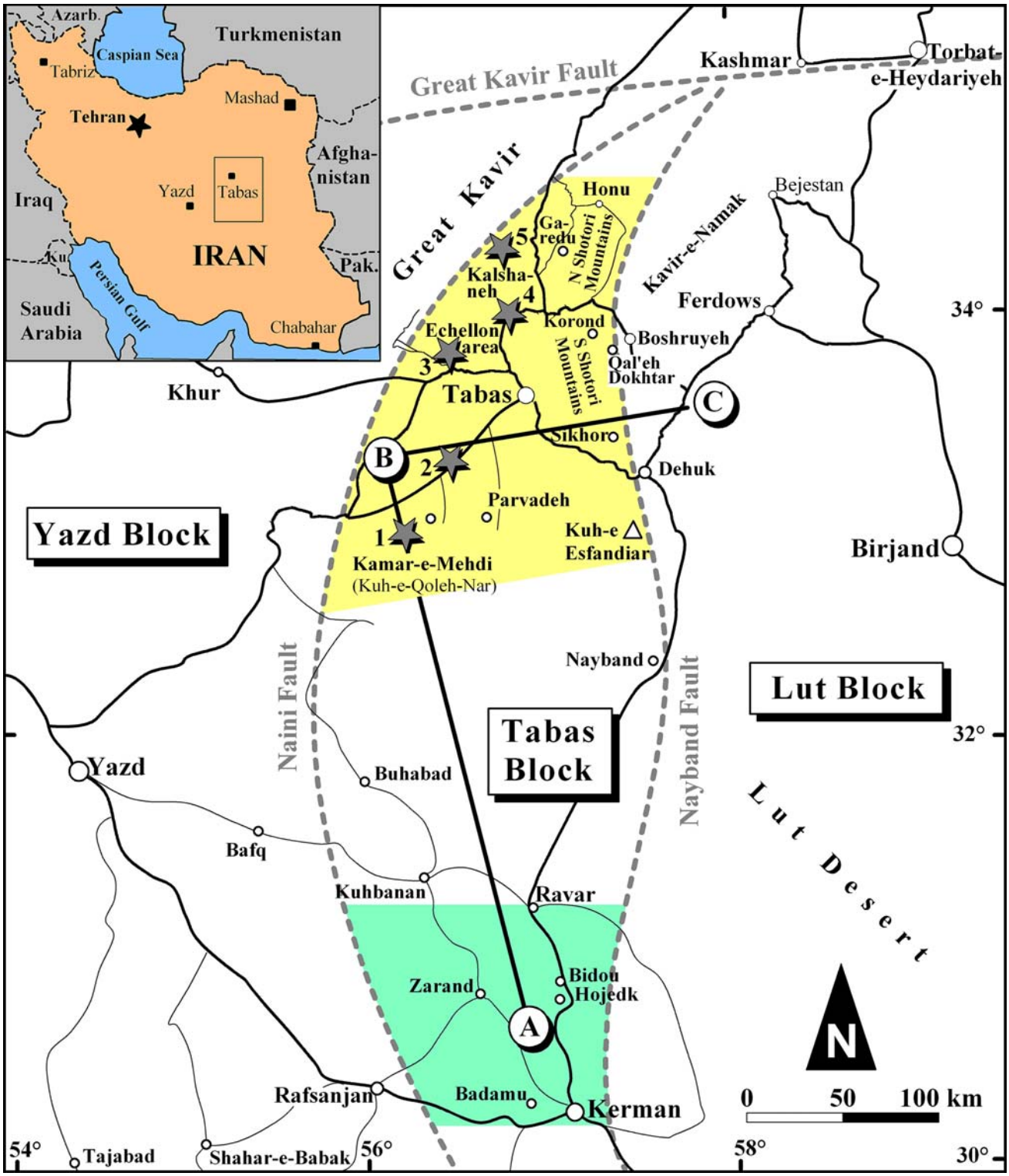

Fig. 1 Locality map of east-central Iran with major structural units (blocks and block-bounding faults; modified from Wilmsen et al. 2009a). The study area is shaded in *yellow* and measured sections are indicated by *asterisks*. *1* Kamar-e-Mehdi type section. *2* Road section ca. 45 km southwest of Tabas. *3* Echellon section. *4* Kuh-e-Bagh-e-Vang section. *5* Kalshaneh section. The lithostratigraphic S–N–E cross section of Fig. 3 is shown (*A–B–C*). The Ravar-Kerman area is shaded in *green*

of the Esfandiar Subgroup (Wilmsen et al. 2003). Its large dimensions (parallel to strike in the order of hundreds of kilometers and perpendicular to it up to 100 km) and superb exposures make it an outstanding example of a Mesozoic shelf-lagoon. Furthermore, the type section of the Kamar-e-Mehdi Formation is re-described herein and the Echellon

and Nar Limestones members are formalized by providing detailed type sections.

In order to document the facies development and evolution of the Kamar-e-Mehdi Formation, five sections were measured bed-by-bed using a modified Jacob Staff (Sdzuy and Monninger 1985). The rocks were investigated in the field by hand lens, sampled for microfacies analysis (more than 200 thin-sections and polished slabs) and classified according to depositional texture (Dunham 1962; Embry and Klovan 1972). Macrofaunal occurrences and ichnological observations as well as sedimentary structures and bedding features (thickness trends, cycles) were recorded and integrated into the facies analysis.

Plate tectonic and palaeogeographic framework

The study area is located in the central part of the Central-East Iranian Microcontinent (CEIM). The CEIM, together with NW Iran and the Alborz Mountains, forms the Iran Plate, which occupies a structural key position in the Middle Eastern Tethysides (Sengör et al. 1988; Sengör 1990). As an element of the Cimmerian microplate assemblage it became detached from Gondwana during the (Late) Permian and collided with Eurasia (Turan Plate) in the Late Triassic, thereby closing the Palaeotethys (e.g., Stampfli and Borel 2002; Wilmsen et al. 2009b). The CEIM consists of three N to S-oriented structural units, called Lut, Tabas, and Yazd Blocks (Fig. 1), that today are aligned from E to W with N to S-trending block-bounding faults (Nayband and Naini faults). The lateral relationships of the three blocks during the Jurassic Period, however, are still under debate since an anticlockwise rotation of about 135° since the Triassic was inferred for the CEIM (e.g., Soffel et al. 1996), but this rotation should have taken place mainly in post-Jurassic (possibly Cenozoic) times (Esmaeily et al. 2007; Bagheri 2008; Bagheri and Stampfli 2008; Wilmsen et al. 2009a). However, even though having being accreted to the southern margin of Eurasia at the end of the Triassic Period (Wilmsen et al. 2009b), the Iran Plate remained a structurally complex and tectonically active area throughout the Mesozoic. This tectonic instability also governed the Jurassic sedimentation pattern in the study area and is reflected in numerous sedimentologic and stratigraphic signatures (Fürsich et al. 2003b, 2009; Wilmsen et al. 2003, 2009a; Seyed-Emami et al. 2004a). The most prominent examples for this tectonic instability are the Mid- and Late Cimmerian tectonic events in the mid-Bajocian and Late Jurassic–earliest Cretaceous, which are documented by conspicuous inter-regional, in part angular unconformities across the Iran Plate. Their origin can be related to plate tectonic processes in the South Caspian area (Brunet et al. 2003; Fürsich et al. 2009) and at the southern margin of the Iran Plate (Wilmsen et al. 2009a). On the Tabas Block, the Mid-Cimmerian unconformity is well developed and associated with considerable erosion and mild folding whereas the Late Cimmerian Event was characterized by intensive block-faulting (Wilmsen et al. 2003, 2009a). Regional tectonic events are documented by fault-related deposition of coarse-grained siliciclastic units such as the Lower Callovian Sikhor Formation (Fürsich et al. 2003b).

Palaeogeographic reconstructions for the Late Jurassic (e.g., Enay et al. 1993; Thierry 2000; Fig. 2) place the Iran Plate at the northern margin of the Neo-Tethys at a subtropical palaeo-latitude of ca. 20°–30°N. Sedimentological and stratigraphical analyses (i.e., distribution of marine strata) indicate that the Tabas and Lut blocks were mostly covered by the sea during the Jurassic Period whereas the Yazd Block remained emergent (Middle Jurassic stratigraphic gap and Upper Jurassic continental clastics). After a short phase of uplift and widespread erosion associated with the Mid-Cimmerian tectonic movements in the Bajocian (e.g., Seyed-Emami and Alavi-Naini 1990; Fürsich et al. 2009), rapid subsidence caused a pronounced transgression as indicated by the onlap of the widespread condensed microbial and ammonite-bearing limestones of the Upper Bajocian-Lower Bathonian Parvadeh Formation and the subsequent deposition of the thick and uniform marly to silty deeper shelf sediments of the Bathonian Baghamshah Formation across the Tabas and Lut blocks (Fig. 3). Uplift and concomitant erosion of the eastern margin of the Tabas Block in the Early Callovian due to rotation of the Tabas Block caused the deposition of the fluvio-deltaic sediments of the Sikhor Formation (Fürsich et al. 2003b), and the resulting N/S directed "Shotori Swell" became the site of a fault-block carbonate platform (Esfandiar Limestone Formation), bordered by slope and basinal areas towards the east (Lut Block). On the western Tabas Block, however, a large-scale shelf-lagoon developed, delimited by the emergent Yazd Block in the west and sheltered by the barrier of the Esfandiar Platform from the open sea. The sedimentary rocks of this depositional system, the Kamar-e-Mehdi Formation, are the focus of this paper.

Stratigraphy

Lithostratigraphy

Lithostratigraphic subdivision of the Middle and Upper Jurassic rocks in the study area is complicated by rapid lateral facies changes and the occurrence of very similar, but stratigraphically clearly different rock units (e.g., the Baghamshah and Korond Formations; Schairer et al. 2003). These difficulties led to considerable misinterpretations during the early mapping surveys (e.g., Stöcklin et al. 1965; Ruttner et al. 1968). Consequently, a completely

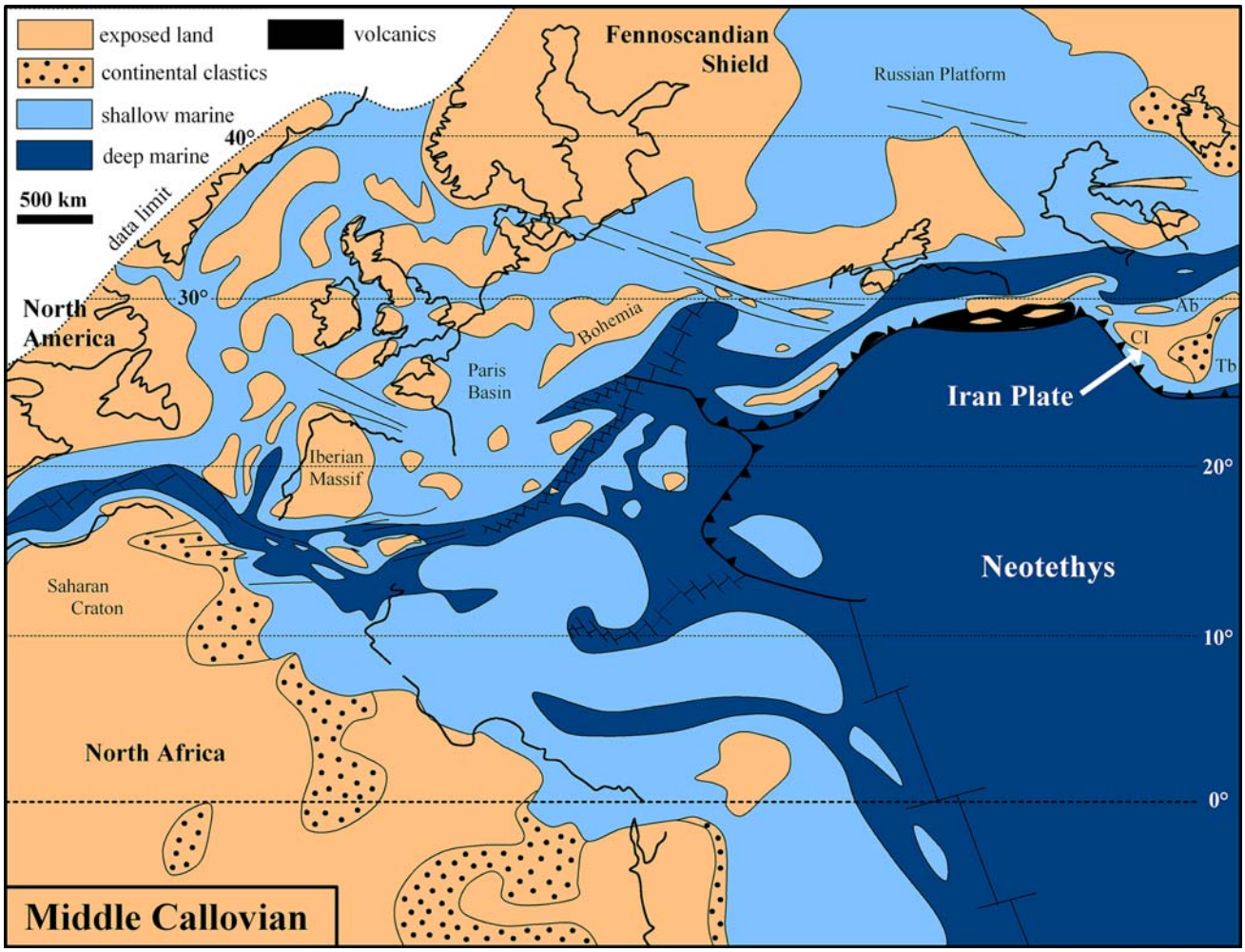

Fig. 2 Callovian palaeogeography of the central and western Tethys (modified after Thierry 2000). *Ab* Alborz, *CI* Central Iran, *Tb* Tabas

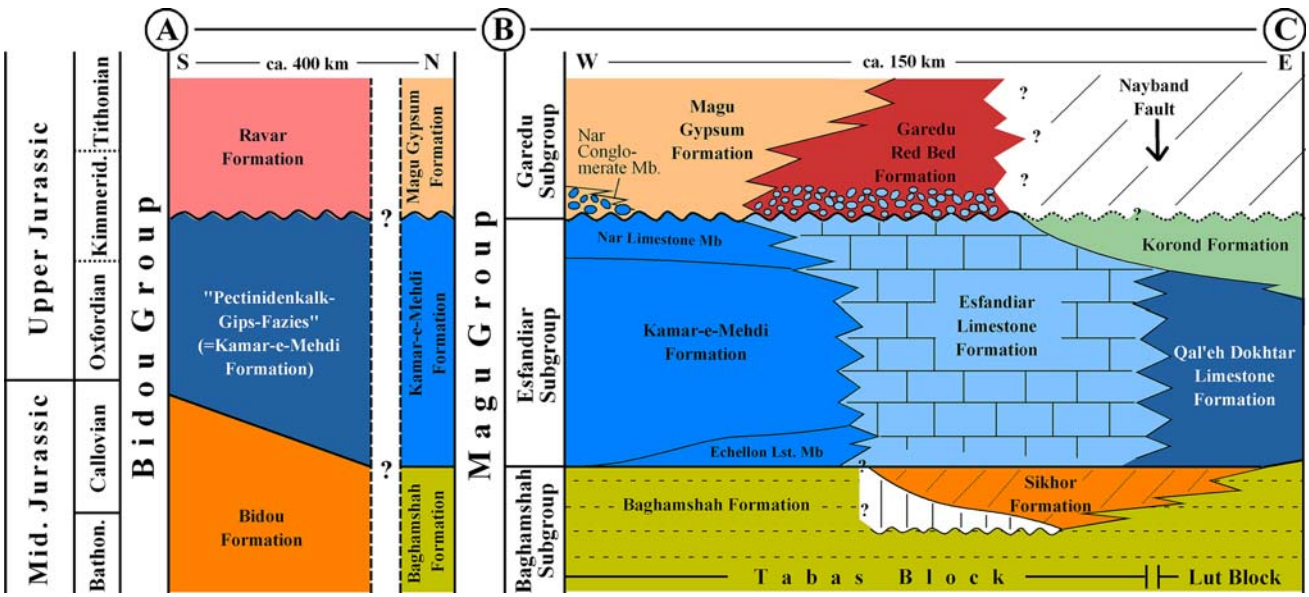

Fig. 3 Lithostratigraphic framework of the Upper Middle and Upper Jurassic of the Tabas Block, east-central Iran. For approximate location of cross section *A–B–C*, see Fig. 1. *A–B* south–north cross-section from the Ravar-Kerman to the Tabas area. *B–C* west–east cross-section of the Esfandiar Subgroup in the northern part of the Tabas Block and the western Lut Block (modified from Wilmsen et al. 2003, 2009a)

revised lithostratigraphy was proposed that strongly simplifies the tectonic structure of the working area (Wilmsen et al. 2003, 2009a). The Middle-Upper Jurassic Magu Group of the northern Tabas Block was subdivided into three subgroups, i.e., the Baghamshah, Esfandiar, and Garedu subgroups (Fig. 3). The subgroups were defined on the basis of (inter-)regional tectonic unconformities and/or conspicuous, widespread facies changes. In an east–west direction (Fig. 3), the Bathonian–Lower Callovian Baghamshah Formation (belonging to the Baghamshah Subgroup) is overlain by an array of calcareous formations (Korond Formation, Qal'eh Dokhtar Limestone Formation, Esfandiar Limestone Formation, Kamar-e-Mehdi Formation) which have been combined to the Callovian to Lower Kimmeridgian Esfandiar Subgroup. In the Kamar-e-Mehdi Formation, a basal Echellon and a capping Nar Limestone Member are distinguished.

The contemporaneous lithostratigraphic units in the southern part of the Tabas Block (Ravar-Kerman area, Fig. 1) are combined in the Bidou Group (see Wilmsen et al. 2009a; Fig. 3). The equivalent unit of the Kamar-e-Mehdi Formation in this area is the "Pectinidenkalk-Gips-Fazies" of Huckriede et al. (1962).

Biostratigraphy

The biostratigraphic subdivision of the Esfandiar Subgroup is mainly based on ammonites (Seyed-Emami et al. 1991, 1997, 1998, 2001, 2002, 2004b; Schairer et al. 2000, 2003). The ammonite faunas allow a fairly precise correlation with the European Standard Biozonation.

The base of the Kamar-e-Mehdi Formation is of Early Callovian age, according to finds of ammonites of the genus *Macrocephalites* (e.g., at Kuh'e Echellon, where the Echellon Limestone overlies the Baghamshah Formation). A similar age can be inferred for the bases of the Qal'eh Dokhtar and Esfandiar Limestone Formations in the east, indicating a broadly synchronous onset of calcareous deposition across the northern Tabas Block. From the Kamar-e-Mehdi Formation itself, only a few and poorly preserved ammonites were collected (Middle Callovian reineckeids, long-ranging perisphinctids). However, the Nar Limestone Member capping the Kamar-e-Mehdi Formation can be dated by means of agglutinated foraminifera just below the Magu Gypsum Formation (Garedu Subgroup) in the Echellon area: *Alvesosepta personata* (Tobler), *A.* ex gr. *personata-powersi*, *A.* cf. *praelusitanica* (Maync), and *Everticyclammina* cf. *virguliana* (Koechlin) indicate a Late Oxfordian to Early Kimmeridgian age (cf. Hottinger 1967; Bassoullet 1997). This is, again, coeval to ammonite data for the top of the Esfandiar Formation in the east (Late Oxfordian to Early Kimmeridgian; see Schairer et al. 2003) and biostratigraphic data from north of the type area of the Esfandiar Formation (Fig. 1) where Bagi and Tasli (2007) inferred a Middle Oxfordian to Early Kimmeridgian age based on benthic foraminifera. The sediments of the overlying Garedu Red Subgroup are difficult to date by means of biostratigraphy. However, Ruttner et al. (1968) reported Kimmeridgian to Tithonian calcareous algae from the Garedu Red Beds of the Garedu area, northern Shotori Mountains (Fig. 1).

The Kamar-e-Mehdi Formation

The Kamar-e-Mehdi Formation represents the Esfandiar Subgroup in the central and western part of the Tabas Block. In most areas of the northern Tabas Block (e.g., Kalshaneh, Echellon area, Figs. 1, 3), two members can be separated within the formation: a basal Echellon Limestone Member and a capping, cliff-forming Nar Limestone Member (Wilmsen et al. 2003), embracing a thick unit of "normal" Kamar-e-Mehdi Formation. In the southern part of the Tabas Block, the Kamar-e-Mehdi Formation is represented by the "Pectinidenkalk/Gips-Fazies" of Huckriede et al. (1962), a more evaporitic facies equivalent of the formation (see below and Figs. 1, 3; Wilmsen et al. 2009a).

Distribution

The Kamar-e-Mehdi Formation is widespread in the western part of the Tabas Block, forming a discontinuous outcrop belt that extends from north of Kalshaneh to the type area at Kamar-e-Mehdi in the south and beyond (being represented by or interfingering with the "Pectinidenkalk/Gips-Fazies" in the Ravar area, north of Kerman, ca. 200–300 km to the south of the study area). In the Kuh-e-Bagh-e-Vang section (see below), an interfingering of the Kamar-e-Mehdi and the contemporaneous Esfandiar Limestone Formation can be demonstrated. The Kamar-e-Mehdi Formation also occurs in the area close to the Naini Fault (Fig. 1), representing the boundary between the Tabas and the Yazd Block. On the Yazd Block, Middle Jurassic rocks are absent and Upper Jurassic strata are represented by terrestrial sediments of the Chah Palang Formation (Aistov et al. 1984, pers. obs.). Thus, the Kamar-e-Mehdi Formation must pinch out, or grade into non-marine rocks, towards the west.

Lithology

The Kamar-e-Mehdi Formation is characterized by a basal Echellon Limestone Member, a thick middle part, and a capping Nar Limestone Member. In the southwestern part of the study area, a siliciclastic unit is intercalated between the Baghamshah and the Kamar-e-Mehdi Formations

(Aghanabati 1998). Its thickness and grain size increases towards the southwest (i.e., towards the Naini Fault representing the boundary to the Yazd Block), and the color changes to red. Unfortunately, due to the poor accessibility of that very remote area, this interesting locality could not be studied. However, it is very likely that this coarse siliciclastic unit is equivalent to a contemporaneous lithostratigraphic unit known from the southern Shotori Mountains, the Sikhor Formation (Fürsich et al. 2003b).

The Echellon Limestone Member is an up to 180-m-thick marly-calcareous unit. It is dominated by dark colors, muddy fabrics (marls, mud-/wackestones, floatstones, and muddy rudstones). Furthermore, it is fairly fossiliferous (oysters, brachiopods, crinoids, siliceous sponges) and particularly rich in microbialites and oncolites.

The middle and major part of the Kamar-e-Mehdi Formation is a thick monotonous succession of marls, marly limestones, limestones and shell beds as well as thin intercalations of mostly sharp-based, parallel-laminated, ripple- or hummocky-bedded silt- to fine-grained sandstones. The succession is characterized by meter-scale, stacked asymmetric cycles (Figs. 4a, c, 5) grading from marl at the base via marly limestone to limestone containing bivalves and other fossils at the top (see below). The most conspicuous faunal elements are large pectinid bivalves (see below). Therefore, lateral equivalents of the Kamar-e-Mehdi Formation in the Kerman area were termed "Pecten-Kalk" by Huckriede et al. (1962), and Aghanabati (1977: 144–148) adopted this informal name ("calcaire a Pectens") for the formation. Often, a cycle is capped by a thin (1–10 cm) winnowed shell bed showing oscillation ripples and encrusted components (Fig. 4f). Intercalated are patch reefs formed by oysters (*Nanogyra nana*), calcareous sponges, and several species of corals (see Pandey and Fürsich 2003 and below for details; Fig. 4d). The dimensions of the bioherms vary from a few decimeters to a few tens of meters. Coral patch reefs built by coral framestones associated with minor contribution of clotted microbialites occur in the lower part of the Kamar-e-Mehdi Formation about 45 km southwest of Tabas (N 33°20′00″, E 56°32′38″). In the upper part of the Kamar-e-Mehdi Formation at the type section, a thick (tens of meters) interval of gypsum and intercalated thin mudstone layers occurs. These evaporitic sediments pinch out towards the northern outcrop areas. Towards the Ravar/Kerman area, south of the study area, gypsum beds prevail throughout the Kamar-e-Mehdi Formation (e.g., Huckriede et al. 1962, and own observations).

The Nar Limestone Member is a bipartite limestone unit with a marly middle part in typical facies of the underlying Kamar-e-Mehdi Formation (Fig. 4g). The limestones are thin- to medium-bedded and fine-grained, and muddy fabrics prevail. The thickness of the Nar Limestone Member is on the order of 80–100 m. The member is cliff forming, capping the predominantly soft-weathering middle part of the Kamar-e-Mehdi Formation (Fig. 4a). The soft clay–gypsum intercalations of the Magu Gypsum Formation follow with a sharp contact (Fig. 4h).

Fig. 4 Field aspects of the Kamar-e-Mehdi Formation. **a** Upper part of the type section at Kuh-e-Koleh-Nar. Note the cyclic pattern of the formation and the cliff-forming terminal Nar Limestone Member. **b** Oscillation ripples on a bedding surface in the type area. **c** Small-scale, 2 to 3-m-thick, asymmetric cycles characterized by increasing carbonate contents; upper part of the formation in the type area. **d** Small lenticular coral patch reef in the lower part of the formation, road section ca. 45 km southwest of Tabas. **e** *Rhizocorallium irregulare* from the lower part of the type section; positive hyporelief (lens cap is 65 mm in diameter). **f** Shell lag (winnowed concentration) on top of shallowing-upward cycle; lower part of the type section (lens cap is 65 mm in diameter). **g** Nar Limestone Member at Kuh-e-Koleh-Nar. Note the tripartite character of the member with two limestone packages separated by a marl unit. **h** Sharp contact between the Nar Limestone Member and the overlying, soft-weathering clay–gypsum facies of the Magu Gypsum Formation at Kuh-e-Koleh-Nar

Sections

Five sections of the Kamar-e-Mehdi Formation were measured in the northern part of the Tabas Block (Fig. 1). These include the type section of the formation which is located between Kamar-e-Mehdi and Kuh-e-Qoleh Nar in the southern part of the study area (Sect. 1 in Fig. 1, N 33°01′10″, E 56°26′36″; see also Aghanabati 1977). Here, the formation reaches a thickness of 1,356 m. Kuh-e-Qoleh Nar is also the type locality of the Nar Limestone Member. At the road from Tabas to Yazd (N 33°20′00″, E 56°32′38″), a 165-m-thick section of the lower part of the formation was measured (Sect. 2). The reference section of the Kamar-e-Mehdi Formation in the northern part of the study area is in the Echellon area (N 33°49′04″, E 56°36′19″) where a 1,200-m-thick section was logged, including the type section of the basal Echellon Member (Sect. 3). The section of Kuh-e-Bagh-e-Vang (N 33°56′54″, E 56°47′05″, Sect. 4) is located north of Tabas and ca. 800 m thick. It is an important section since it is the only section where the hitherto only inferred interfingering of the Esfandiar Limestone and Kamar-e-Mehdi Formations can be observed. The northernmost occurrence of the Kamar-e-Mehdi Formation is at Kalshaneh (Fig. 1, N 34°08′54″, E 56°41′16″), where only the lower part of the formation is exposed in the core of a syncline. Thus, only the 110-m-thick basal Echellon Member was logged. In order to keep this account short, only the type section of the formation, the type section of the Echellon Member, and the section at Kuh-e-Bagh-e-Vang are figured herein and described in more detail below (Figs. 5, 6, 7).

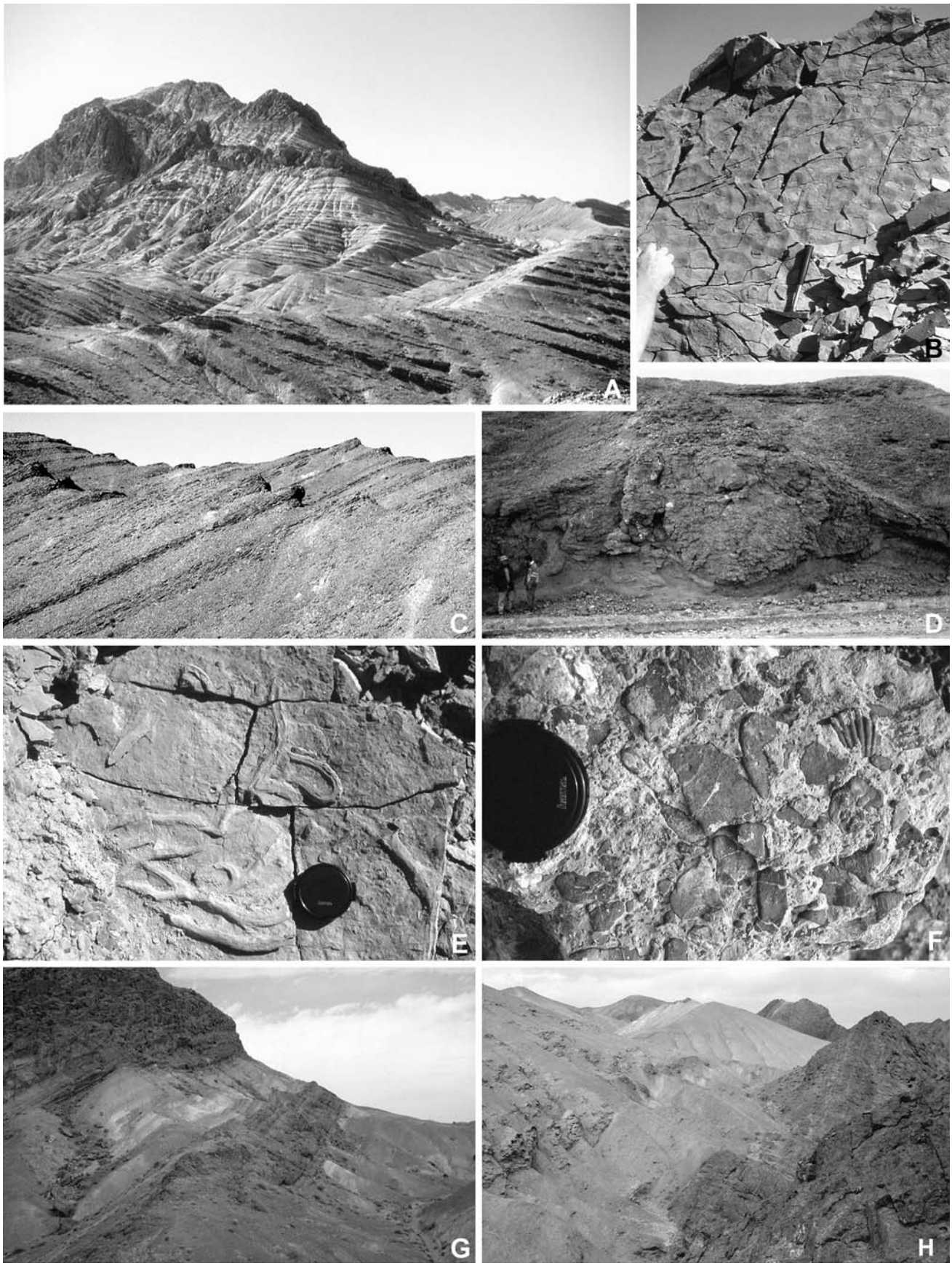

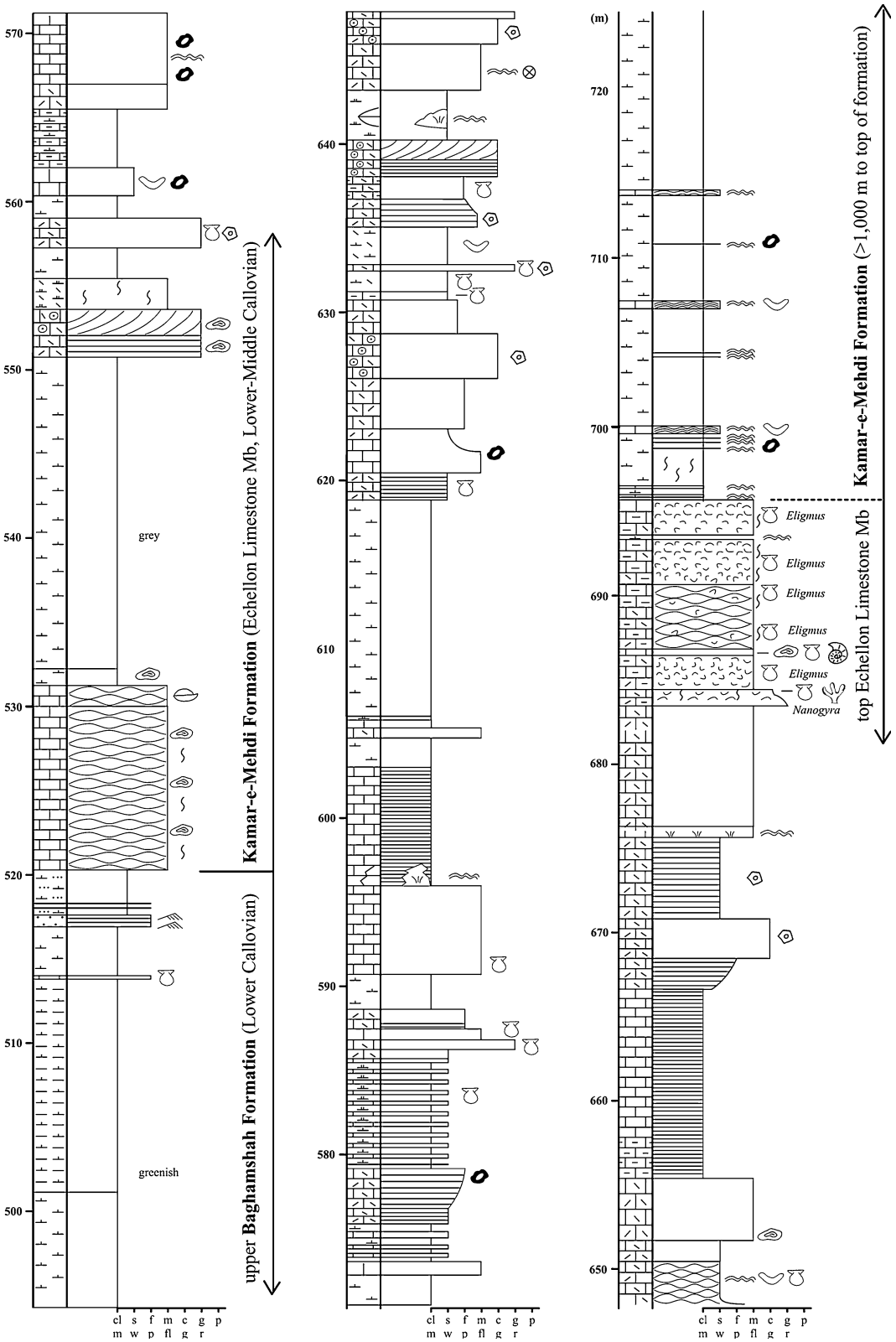

Fig. 5 Type section of the Callovian Echellon Member of the Kamar-e-Mehdi Formation in the Echellon area (N 33°49′04″, E 56°36′19″). For key of symbols see Fig. 7

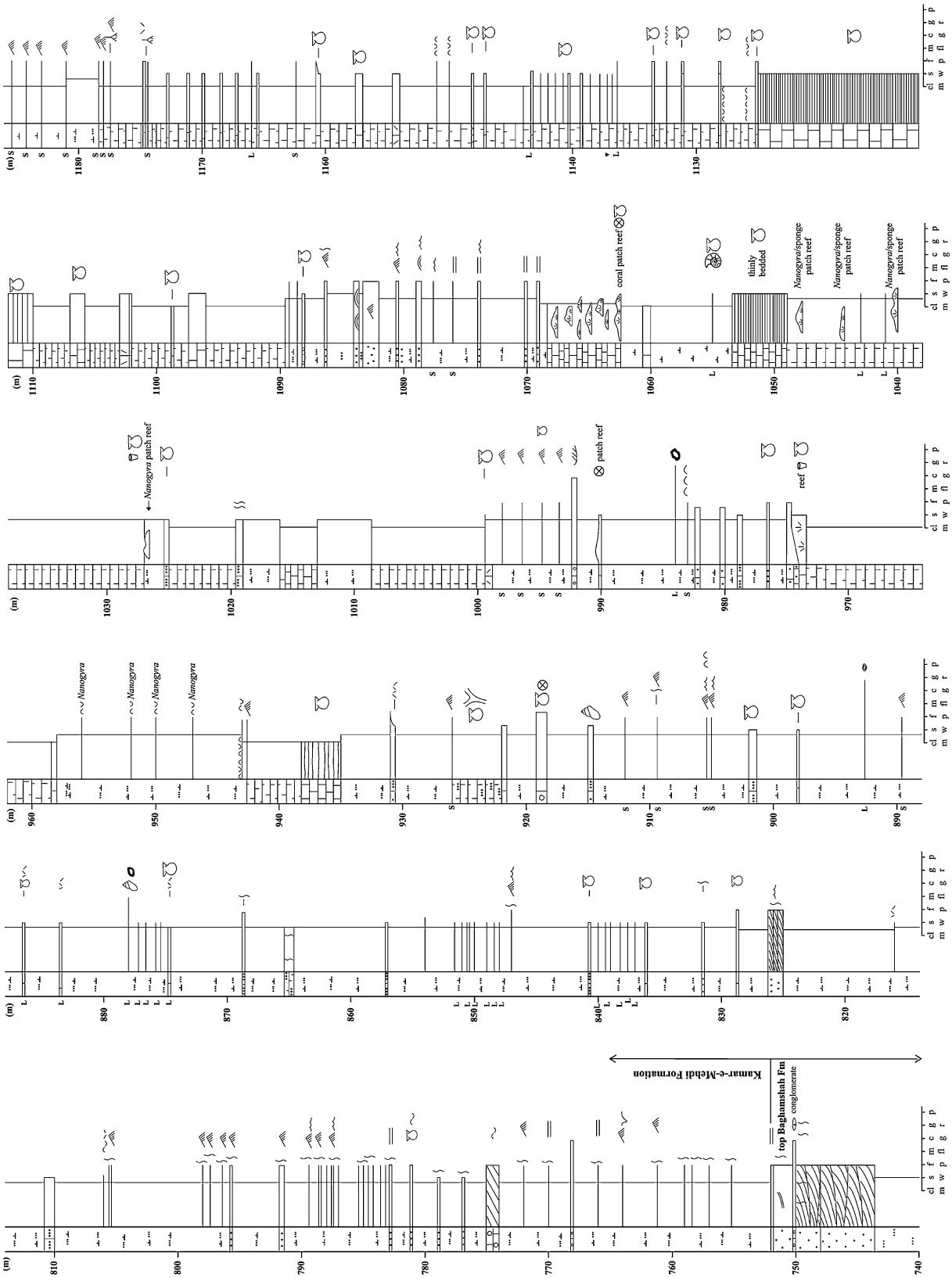

Fig. 6 Type section of the Callovian to Lower Kimmeridgian Kamar-e-Mehdi Formation between Kamar-e-Mehdi and Kuh-e-Qoleh Nar (N 33°01′10″, E 56°26′36″). For key of symbols see Fig. 7

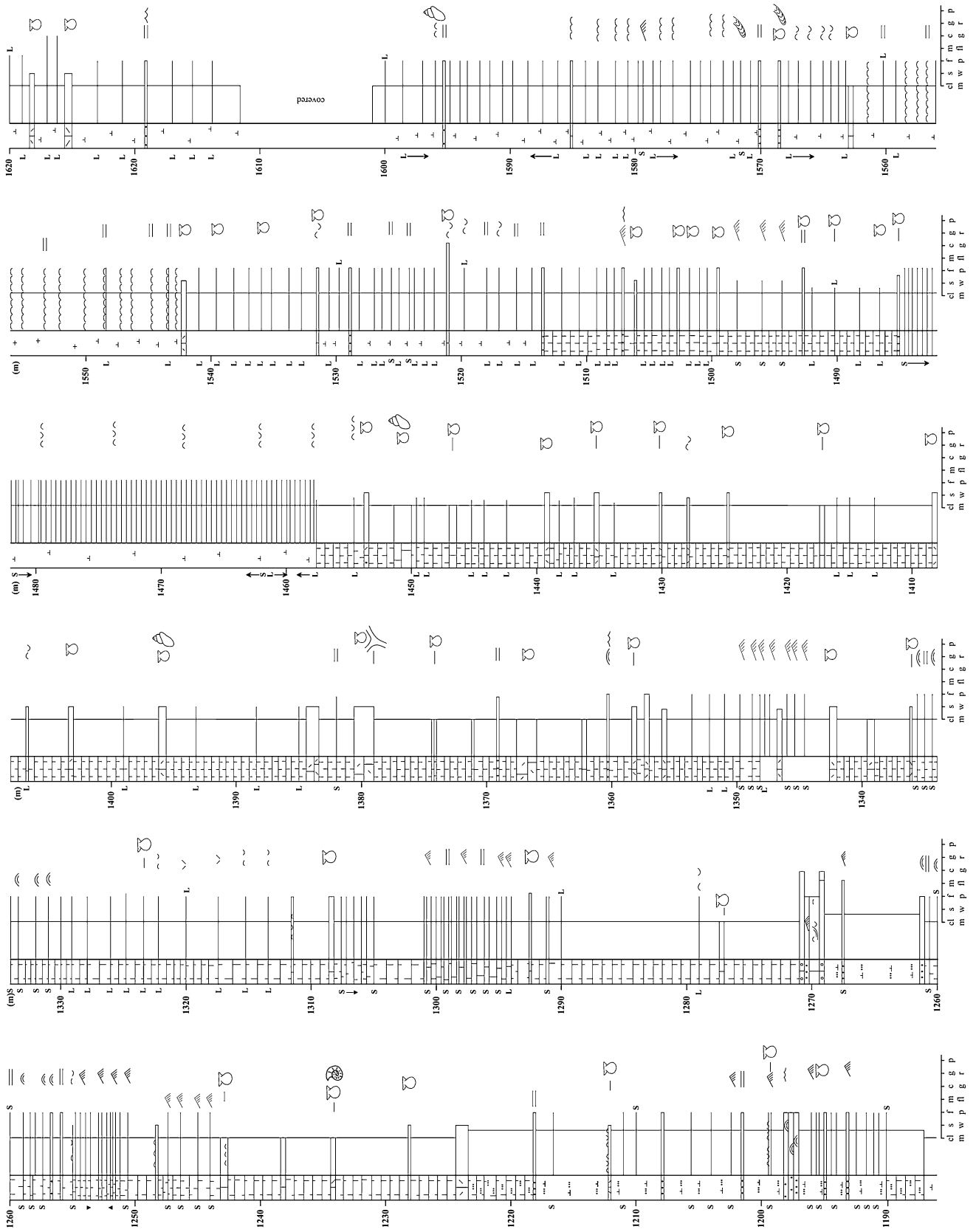

Fig. 6 continued

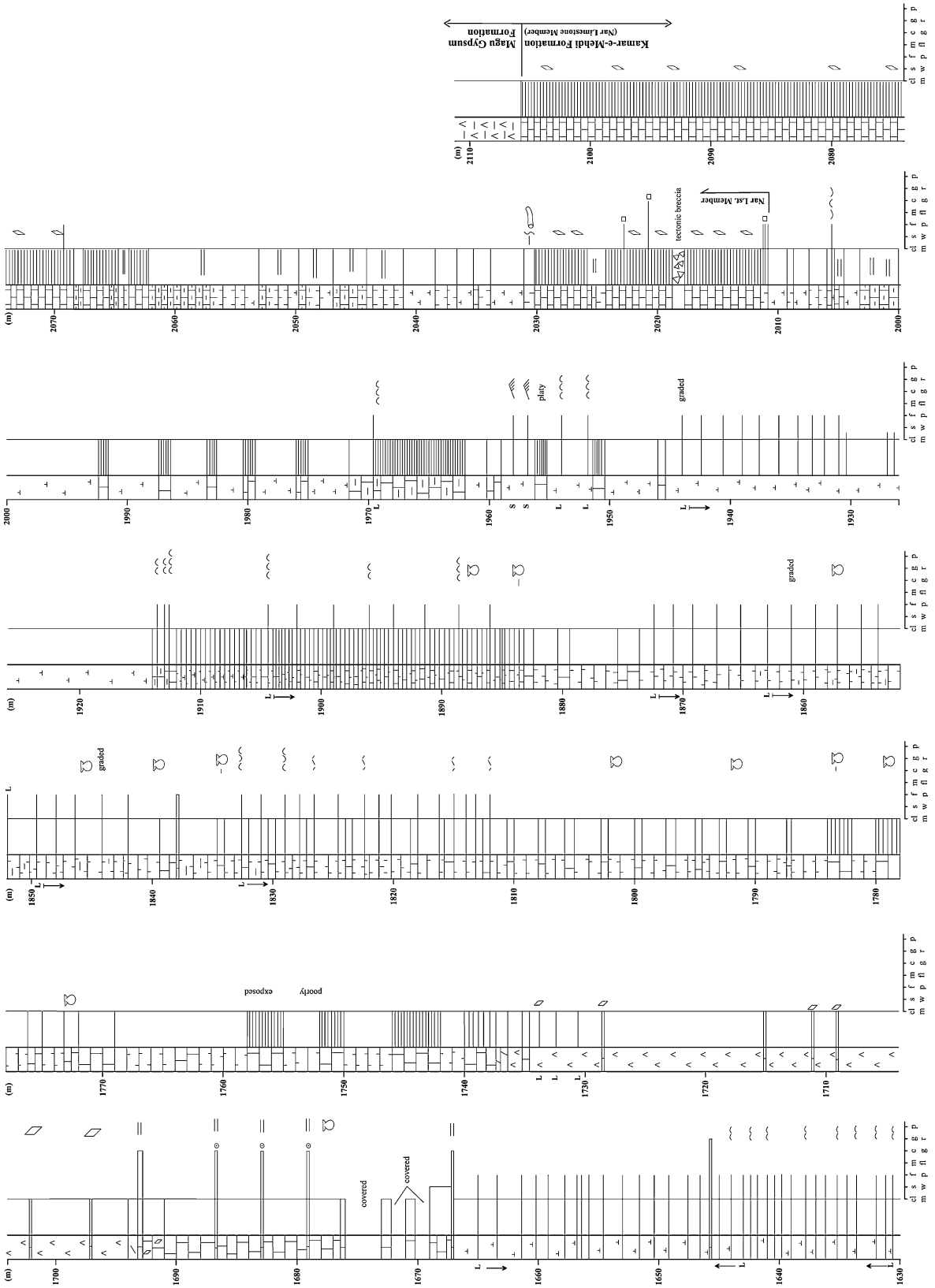

Fig. 6 continued

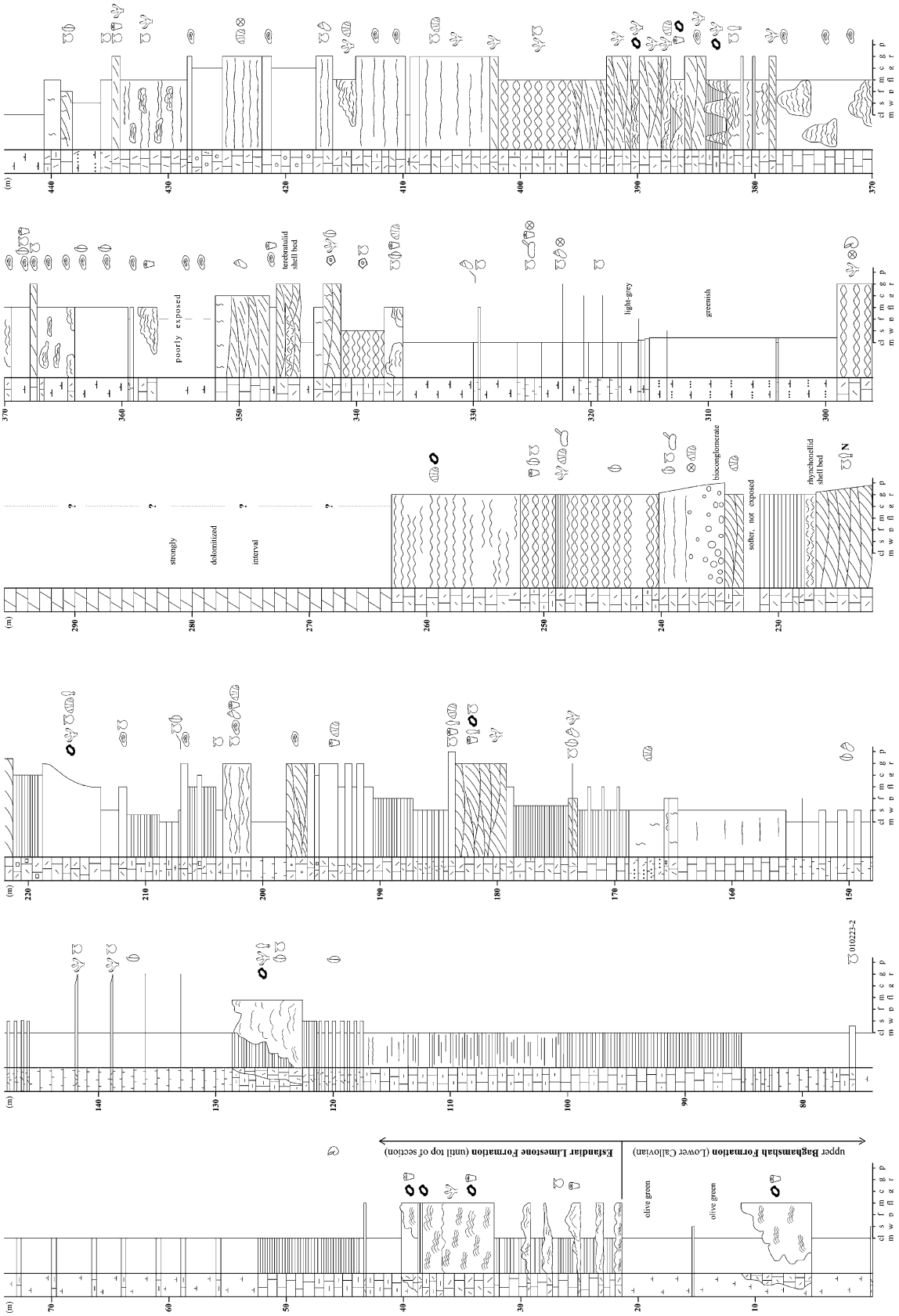

Fig. 7 Section at Kuh-e-Bagh-e-Vang (N 33°56′54″, E 56°47′05″) showing the interfingering of the Kamar-e-Mehdi and Esfandiar Limestone Formations. Key of symbols applies for all other figures

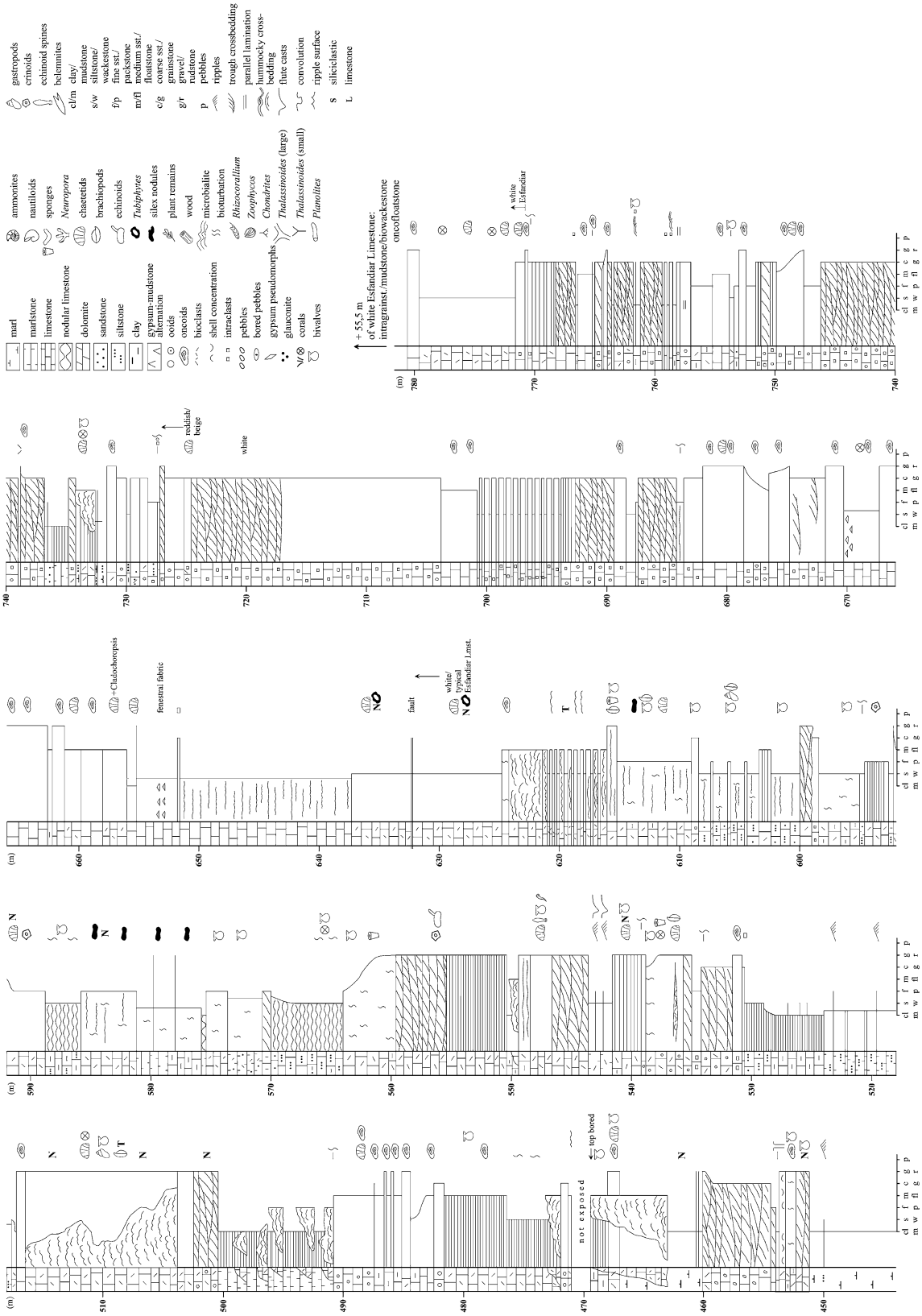

Fig. 7 continued

Echellon area

The section of the Kamar-e-Mehdi Formation in the Echellon area was measured across Kuh-e-Echellon, the type locality of the Echellon Limestone Member. It is underlain by about 450 m of greenish marls of the Baghamshah Formation which, based on ammonite evidence, has a Late Bathonian to Early Callovian age at this locality. The Echellon Limestone Member is 175 m thick and starts with a thick unit of oncoid floatstone followed by ca. 20 m of grey marls (Fig. 5). The remaining succession is composed of an intercalation of bioclastic, occasionally oolitic grain- and rudstones, oyster floatstones, stratiform and lenticular microbialites, and fine-grained marly limestones and marls. Nodular fabrics are common and the succession is fairly fossiliferous (oysters, siliceous sponges, crinoids, brachiopods, some microsolenid corals). At the top of the Echellon Limestone Member, a succession of shelly floatstones with abundant *Eligmus* sp. is developed. The boundary to the overlying middle part of the Kamar-e-Mehdi Formation is relatively sharp, and microbialite beds characterize the lowermost part of this unit. The thickness of the complete formation is 1,200 m at this locality. Near the top, in the upper part of the Nar Limestone Member, an assemblage of benthic foraminifers (*Alveosepta personata*, *A*. ex gr. *personata-powersi*, *A*. cf. *praelusitanica, Everticyclammina* cf. *virguliana*) indicates the latest Oxfordian–Early Kimmeridgian (see above). The Kamar-e-Mehdi Formation is overlain by red gypsiferous sand- and siltstones of the Magu Gypsum Formation containing an 8 to 10-m-thick, clast-supported, coarsening-upward conglomerate containing well-rounded Nar Limestone pebbles and cobbles (Nar Conglomerate Member; Seyed-Emami et al. 2004a).

Kamar-e-Mehdi area

The type section of the Kamar-e-Mehdi Formation (no. 1 in Fig. 1) provides a continuous and very thick succession from the underlying Baghamshah to the overlying Magu Gypsum Formation in the southwestern part of the study area (Fig. 6). No basal Echellon Limestone Member is developed, but the formation starts above a cross-bedded, 8-m-thick sandstone bed assigned to the top of the Baghamshah Formation. In the upper part of this sandstone unit, a thin conglomerate consisting of partly bored sandstone and limestone clasts occurs. Up-section, the typical fine-grained marly-calcareous facies with intercalated bivalve shell layers and fine-grained sandstone beds as well as scattered patch reefs of corals and *Nanogyra*-calcareous sponges prevails which characterizes the middle part of the formation also in the northwestern area. In the lower part, the marls tend to contain some silt. Between 970 and 1,090 m of the section, patch reefs dominated by corals or *Nanogyra* and calcareous sponges are common. Noteworthy is the thick intercalation of gypsum with intercalated mudstone beds between 1,694 and 1,736 m of the section (Fig. 6). The upper part of the formation is completely dominated by the fine-grained marly-calcareous facies and much less fossiliferous compared to the lower part. This trend continues in the terminal Nar Limestone Member, which is 95 m thick at its type locality at Kuh-eh-Qoleh-Nar and devoid of macrofossils. The boundary to the overlying reddish gypsum–clay intercalations of the Magu Gypsum Formation is very sharp.

Kuh-e-Bagh-e-Vang

The section at Kuh-e-Bagh-e-Vang (Sect. 4 in Fig. 1) is the only one demonstrating the interfingering of the Kamar-e-Mehdi and Esfandiar Limestone Formations (Fig. 7). This interfingering has been postulated based on the contemporaneous deposition of both units (Callovian to Late Oxfordian-Early Kimmeridgian; Fürsich et al. 2003a; Schairer et al. 2003; Wilmsen et al. 2003) but the N to S-trending zone where it must take place is located in the Tabas desert plain where Mesozoic rocks are covered by thick successions of Neogene siliciclastic sediments. As the outcrop at Kuh-e-Bagh-e-Vang is mapped as Esfandiar Limestone Formation (Stöcklin et al. 1965), the succession is lithostratigrapically kept within this formation.

The section starts with greenish marls of the upper Baghamshah Formation which yielded Early Callovian ammonites (*Macrocephalites* sp.). The lower part of the section between 21.5 and 175 m is similar to the Echellon Limestone Member of the Kamar-e-Mehdi Formation because of intercalations of microbial build-ups and grey, fine-grained marls and limestones (Fig. 7). Up-section, the succession is dominated by thick, in part large-scale trough-crossbedded, oolitic-bioclastic limestone (grain- and rudstones), oncolitic floatstones, microbial patches and shell beds alternating with up to 35-m-thick units of marl and marly limestone. The small sclerosponge *Neuropora* and chaetetids are very common (such as in the typical Esfandiar Limestone Formation; Fürsich et al. 2003a) and brachiopods are fairly abundant, too (forming two thick autochthonous shell beds at 227 and 346 m of the section). In the upper part, above 625 m, the succession becomes less bioclastic and finer grained. Up to the top, mud-/wackestones, in part with fenestral fabrics, fine intraclast grainstones, oncolitic limestones and cross-bedded oolites predominate. Some mudstone beds show gypsum pseudomorphs reminiscent of the Nar Limestone Member of the Kamar-e-Mehdi Formation.

Microfacies

The stratigraphic succession of the Kamar-e-Mehdi Formation is dominated by ‘muddy’ low-energy sediments (mudstones,

wackestones, floatstones) with only sporadically intercalated high-energy beds (grain- and rudstones) and autochthonous carbonates (framestones, microbialites). The association of a total of 26 facies types (Table 1) is fairly diverse for a lagoonal system and all facies types are listed and briefly described in Table 1 as well as illustrated in Figs. 8, 9, 10. They are mainly based on microfacies analysis, but also include field observations such as bedding characteristics, sedimentary structures, and trace fossils.

The Echellon Limestone Member is characterized by nine facies types (FT 1-9; Table 1). Most of these facies types are characteristic of comparatively deep subtidal environments (e.g., FT 1, 2, 7, 8), some also occur in the more shallow marine, lagoonal middle part of the Kamar-e-Mehdi Formation (e.g., FT 6, 9): Oncoid float- to rudstones (FT 6) characterize the transition from the Echellon Limestone Member to the middle part of the formation in the Echellon area and also occur associated with lagoonal coral patch reefs. The microbialites of FT 7 are also a characteristic feature of the Echellon Member which overall documents open-marine deposition mainly below storm wave-base.

The middle part of the Kamar-e-Mehdi Formation is composed of ten facies types (FT 10–19; Table 1). However, the bulk of this unit is made up of only two fine-grained facies types (FT 11-12, mud- to wackestones) whereas the remaining facies types occur as more-or-less thin intercalations. These include the carbonate build-ups of FT 12 and 13, the winnowed shell beds of cycle tops (FT 15), and the tempestitic intercalations of FT 16–18. Facies types 11 and 12 reflect fine-grained deposition below the fair-weather wave-base in a generally fully marine lagoonal setting. Facies type 19 occurs in thicker units of up to tens of meters consisting of thin-bedded, heterolithic intercalations of gypsum and mudstone layers. This facies type indicates prolonged restricted conditions in the lagoon.

The Nar Limestone Member is characterized by seven, exclusively fine-grained facies types (FT 20–26; Table 1). Pure, in part gypsiferous mudstones (FT 20, 21) and peloidal wacke- to packstones (FT 22–24) predominate. Grainstones occur only as thin, intercalated beds. These facies types testify a low-energy, somewhat restricted peritidal environment punctuated only episodically by high-energy events (storms, high tides).

Macrobiota

The most conspicuous macrofaunal elements are large pectinid bivalves (*Radulopecten*, *Camptonectes*; Fig. 11), which occur abundantly and gave rise to the former (informal) name “Pecten Limestone” for the lithostratigraphic unit (Huckriede et al. 1962; Aghanabati 1977). They are accompanied by a diverse assemblage (ca. 50 taxa) of infaunal and semi-infaunal bivalves such as *Protocardia*, *Anisocardia*, *Nicaniella*, *Corbulomima*, *Ceratomya*, *Homomya*, *Modiolus*, *Arcomytilus,* and *Gervillella* (Fig. 11). The remaining taxa are rare except for the malleid genus *Eligmus* (which is common at the transition from the Echellon Limestone Member into the middle part of the Kamar-e-Mehdi Formation at Echellon) and the small oyster *Nanogyra nana*, which is an important element of small patch reefs. Gastropods are moderately diverse (at least ten taxa), but never occur in large numbers. Corals and calcareous sponges are restricted to patch reefs, which are fairly common in the Echellon Limestone Member. Several species of phaceloid, sheet-like and hemispherical colonial corals as well as solitary corals occur (e.g., *Apocladophyllia, Heliocoenia, Latomeandra, Pseudocoenia, Microsolena,* and *Solenocoenia*; for details see Pandey and Fürsich 2003). Brachiopods, both rhynchonellids and terebratulids, are relatively common in the Echellon Limestone Member. In contrast, ammonites are very rare and represented by only a few fragments of perisphinctids and reineckeids. Bioturbation, however, is very common throughout the succession, in particular the trace fossils *Thalassinoides*, *Rhizocorallium irregulare, Chondrites* and *Planolites* occur (e.g., Fig. 4e).

Small-scale carbonate cycles

A conspicuous feature of the stratigraphic architecture of the Kamar-e-Mehdi Formation (with the exception of the Echellon and Nar Limestone members) are thin (2–4 m), asymmetric cycles characterized by upwards-increasing carbonate content (Figs. 4a, c, 6, 12). They usually start above a basal shell lag with dark-grey, fine-grained marls and marly limestones (mud- to wackestones) that grade upwards into light-grey, fine-grained wackestones capped by a terminal shell bed containing abundant bivalves (see above). These shells may show taphonomic alteration (encrusting, boring, breakage, abrasion; Fig. 4f) but often, the preservation of the bivalves is fairly good and pectinids as well as semi-infaunal bivalves such as modiolids occur with both valves articulated. Intercalated between the fine-grained part of the cycles may be thin (usually less than 10 cm), graded, hummocky cross-stratified or parallel-laminated bioclastic grain-/rudstone or silt- to fine-grained sandstone beds containing oscillation ripples at their tops (Figs. 4b, 9f-i). Bioturbation is common, especially towards the top of the cycles (mainly *Thalassinoides* isp. and *Rhizocorallium irregulare*). The different lithologies of the cycles, soft at the base, harder towards the top, result in saw tooth-like weathering profiles of the formation (Fig. 4a, c). No clear stacking patterns (bundling, thickness trends) have been observed and their numbers have not been counted yet.

Table 1 Facies types of the Kamar-e-Mehdi Formation of east-central Iran

FT	Name	Short description	Interpretation, remarks
Facies types of the Echellon Limestone Member of the Kamar-e-Mehdi Formation			
(1)	Marly wackestones	Mud-supported fine-grained bioclasts (mainly bivalve debris) with inhomogeneous (bioturbated) fabric	Open-marine subtidal deposition below storm wave-base (SWB)
(2)	Filament-bearing wackestones	Mud-dominated fabric with dispersed filaments and small gastropods and crinoid fragments (Fig. 8a, b); may be marly and bioturbated	Open and relatively deep marine sub-SWB deposits
(3)	Shell beds	Oyster and brachiopod boundstone beds (biostromes) with a (marly) fine-bioclastic wackestone matrix	Rare, autochthonous, subtidal shell concentrations
(4)	Bioclastic floatstones	(a) Bioclastic floatstones with irregularly dispersed corals, bivalve, brachiopod and echinoderm debris; strong taphonomic alteration (borings, serpulid and microbial encrustations) (Fig. 8b, c) (b) Similar to type (a) but with oyster dominance (oyster floatstone, Fig. 8d)	Bioturbated, subtidal deposits; floatstone fabric probably due to bioturbation of formerly discrete shell beds
(5)	Bioclastic rudstones	Poorly sorted bioclastic fabric containing *Neuropora*, oysters, siliceous sponges, crinoids, and brachiopods (Fig. 8e)	Subtidal deposit documenting reworking and/or redeposition by storms
(6)	Oncoid float- to rudstones	Contain lobate oncoids up to 10–30 mm in diameter, floating in a mud- to wackestone matrix (Fig. 8f) with variable amounts of bioclasts (bivalves, corals, bryozoans, gastropods, crinoids, brachiopods) and microbial fragments; several oncoids may fuse to form lobate microbial patches of less than 10 cm diameter (cf. FT 7) often associated with serpulid tubes; nodular fabric common	Subtidal, slightly condensed deposits; common in Echellon Limestone Member especially at the top of the type section; also associated with lagoonal coral patch reefs (FT 13, see below)
(7)	Microbialites	dm- to m-scale structures with clotted internal fabrics and encrusting bryozoans, siliceous sponges (Fig. 8h), corals, polychaete tubes, and *Tubiphytes*; often bored by bivalves and clionaid sponges (*Entobia*), in part with rudimentary oncolitic fabrics (Fig. 8g)	Subtidal microbial mounds and patches, common in Echellon Limestone Member; also occurring rarely in lagoon associated with coral patch reefs (FT 13, see below)
(8)	Spiculitic packstones	Densely packed fabric of isolated demosponge spicules (monaxone, tetraxones, rhaxes?) (Fig. 8j)	Relatively rare subtidal deposits associated with microbialites
(9)	Onco- and oolitic bioclastic pack- to grainstones	Slightly irregularly shaped, small oncoids with variable amounts of bioclasts and rare ooids; poorly sorted with inhomogeneous fabric (bioturbation) (Fig. 8h)	Subtidal sediments of elevated water energy, possibly around swells; also in the lagoon during shallowing episodes
Facies types of the Kamar-e-Mehdi Formation			
(10)	Microbioclastic mud- to wackestones	May be marly and contain a few ostracod shells and microbioclasts as well as scattered peloids and silt-sized quartz grains; bioturbation common, e.g., by *Chondrites* isp. (Fig. 9a)	Form the bulk of the fines deposited in the lagoon, representing low-energy conditions below fair-weather wave-base (FWWB)
(11)	Bioclastic wackestones	Most notable are variable amounts of microbioclasts, ostracods, small agglutinating foraminifera, bivalve shells and thin echinoid spines as well as silt-sized angular quartz. Bioturbation present (Fig. 9b)	Represent shallow subtidal low-energy conditions below lagoonal FWWB
(12)	*Nanogyra*/calcareous sponge framestones	The oyster *Nanogyra nana* forms small, up to meter-thick patches associated with calcareous sponges, intercalated between marly mud- to wackestones of FT 10-11 (Fig. 9c)	Small lagoonal patch reefs; gradual transitions to pure *Nanogyra* and calcareous sponge patches exist
(13)	Coral framestone	Phaceloid, sheet-like and hemispherical corals predominate which are often covered by a thin microbial coating; strong bioerosion by lithophagid bivalves (Fig. 9d); laterally grading into oncoid floatstones or mud- and wackestones. Associated elements are regular echinoids (cidarids) and large, thick-shelled *Trichites*, frequently double-valved or even in life position	Form lagoonal patch reefs; dimensions range from small (dm) patches up to patch reefs several meters in thickness and 50 m in width (Fig. 4d) with low relief above the sea floor

Table 1 continued

FT	Name	Short description	Interpretation, remarks
(14)	Bioclastic coral rudstones	Associated with larger coral patch reefs; bioclastic rudstones consisting of coral fragments, cidarid spines, *Trichites* and other bivalve fragments. The fabric is poorly sorted and many components are encrusted, bored, and/or coated by microbial films (Fig. 9e)	Debris aprons of lagoonal patch reefs due to bioerosion and off-reef transport during storms
(15)	Winnowed shell beds	At the top of m-scale carbonate cycles (marly mudstone to mud-/wackestone; Fig. 4c), 1 to 5-cm-thick shell beds occur, containing a moderately diverse assemblage of bivalves and gastropods; components are often encrusted (serpulids), indicating a complex taphonomic history (Fig. 4f)	Winnowed shell concentrations capping lagoonal shallowing-upward cycles
(16)	Sharp-based bioclastic pack- to rudstones	Maximum thickness 10–20 cm, containing bivalve, gastropod and crinoid debris, intercalated between fine-grained sediments and often bundled in certain intervals; ripple bedded at the top. In part silty; originally aragonitic shells as cortoids. Internal fabric either graded (Fig. 9f), or chaotic with concave-up shells and sandfang (Fig. 9g)	Inferred to indicate storm deposition with either lateral transport (graded beds), or in situ reworking by storm waves (shells convex-up with sandfang due to gravitational settling from water column after stirring of sea floor)
(17)	Well-sorted intraclast grainstones	Well-sorted, sharp-based fine-grained intraclasts (~ 0.1 mm Ø) with rare bioclasts and very small foraminifera in thin beds (Fig. 9h)	Distal storm event beds, indicate sediment export off the Esfandiar Platform during storms
(18)	Well-sorted silt- to fine-grained sandstones	Thin (usually 5–10 cm, maximum 20 cm), well-sorted silt- to fine-grained sandstone beds with sharp bases, parallel and ripple bedding (often oscillation ripples at the top), and sometimes hummocky cross-stratification are a rare but persistent feature; occasionally bioturbated by *Chondrites* isp. (Fig. 9i)	Represent siliciclastic tempestites, probably originating from the western margin of the shelf-lagoon (Yazd Block)
(19)	Thin-bedded gypsum-mudstone intercalations	Thick (up to tens of meters) intervals of intercalated thin gypsum and mudstone layers	Evaporitic sediments within the Kamar-e-Mehdi Formation, indicate (semi-) arid conditions and episodic restriction
Facies types of the Nar Limestone Member of the Kamar-e-Mehdi Formation			
(20)	Mudstones	Pure mudstones with rare ostracod shells (Fig. 10c) form the bulk of the Nar Limestone Member	Low-energy peritidal setting, possibly restricted (associated with FT 21)
(21)	Mudstones with gypsum pseudomorphs	Similar to FT 20 but with 1–2 mm long former gypsum needles; may contain rare peloids and small ostracod shells (Fig. 10i)	Evaporitic sediments indicating (semi-) arid climatic conditions and hypersalinity
(22)	Peloidal ostracod wackestones	Peloids and thin-shelled ostracods within a mud-supported fabric (Fig. 10b)	Low-energy shallow peritidal facies
(23)	Peloid grain-/packstone	Well sorted, occasionally with ostracods and agglutinating foraminifera of the genera *Alveosepta* and *Everticyclammina*, bioturbated (Fig. 10a, d, e)	Low- to moderate-energy, shallow subtidal accumulations of fecal pellets, also on tidal flats
(24)	Crustacean coprolite wacke- to packstone	Crustacean coprolites of the *Parafavreina*-type in peloidal wackestone matrix (Fig. 10h)	Low-energy, restricted lagoonal setting
(25)	Bioclastic ooid grainstone	Thin, occasionally graded beds of ooid grainstone with variable amounts of bioclasts (mainly bivalve shells with micritic envelopes); radial-fibrous ooids are commonly small (~500 µm in diameter) and occasionally flattened (Fig. 10f)	Indicating episodes of elevated energy (storms, high tides) within otherwise low-energy peritidal settings; ooids probably formed in low-energy marginal pools
(26)	Bioclastic intraclast grainstone	Thin, occasionally graded beds of intraclast grainstone with a few dispersed bioclasts showing micritic envelopes (Fig. 10g)	Indicating episodes of elevated energy (storms, high tides) within otherwise low-energy peritidal settings

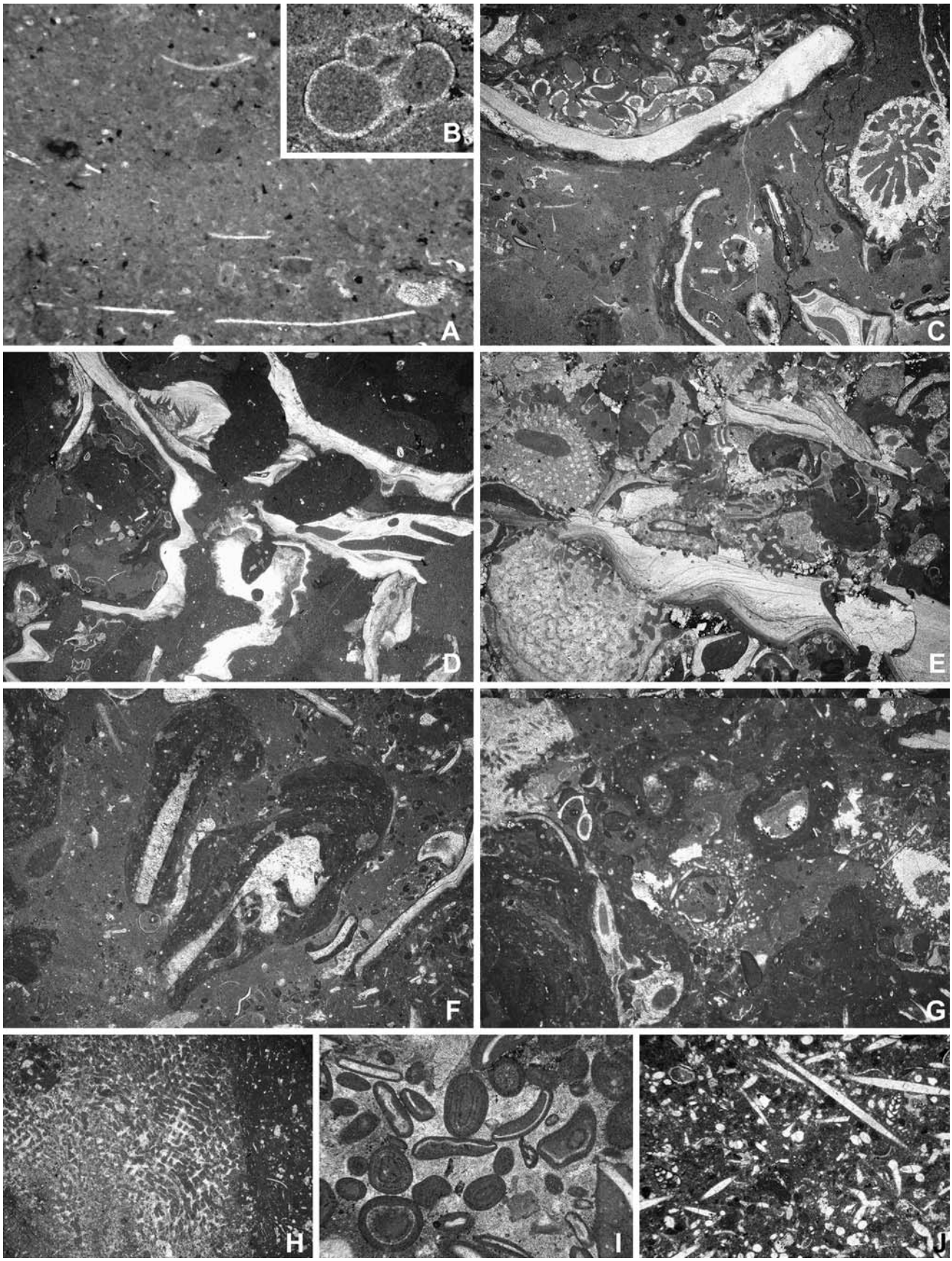

◀ **Fig. 8** Microfacies of the Echellon Limestone Member of the Kamar-e-Mehdi Formation. **a** Filament-bearing microbioclastic wackestone (FT 2). Note diagenetic pyrite (*black grains*). Section at Kuh-e-Bagh-e-Vang, sample 010223-IR19; width of photomicrograph is 2.5 mm. **b** Small gastropod within wackestone of FT 2. Kuh-e-Bagh-e-Vang section, sample 010223-IR19; width of photomicrograph is 1.2 mm. **c** Bioclastic floatstone (FT 4a) with corals, serpulid-encrusted bivalve shells, echinoderm debris, and other microbioclasts. Kalshaneh section, sample 010212-6; width of photomicrograph is 10 mm. **d** Oyster floatstone (FT 4b). Echellon section, sample W34-99; width of photomicrograph is 10 mm. **e** Bioclastic rudstone (FT 5) with *Neuropora*, siliceous sponge, oyster, bivalve and echinoderm debris. Note borings in oyster shell. Kalshaneh section, sample 010212-7; width of photomicrograph is 10 mm. **f** Oncolitic floatstone (FT 6) with lobate oncoids floating in a microbioclastic wackestone matrix. Road to Yazd section, sample 020214-6; width of photomicrograph is 10 mm. **g** Microbialite (FT 7) with microsolenid corals (*upper left*), polychaete tubes and non-rigid demosponge (*right centre*). Echellon section, sample 970218-10; width of photomicrograph is 10 mm. **h** Small hexactinellid sponge occurring within microbialite of FT 7. Echellon section, sample 970218-11; width of photomicrograph is 10 mm. **i** (Micro-)onco- oolitic bioclastic pack- to grainstone (FT 9). Road to Yazd section, sample 020218-10; width of photomicrograph is 2.5 mm. **j** Spiculitic packstone (FT 8). Echellon section, sample W37-99; width of photomicrograph is 2.5 mm

Discussion

Depositional environment

The available facies data (bio-, ichno- and microfacies, sedimentary structures) point to a shallow marine but generally low-energy environment for the bulk of the Kamar-e-Mehdi Formation. Intercalated coral and oyster-calcareous sponge patch reefs as well as oscillation ripples on bedding surfaces suggest fairly shallow conditions (euphotic zone, above the storm wave-base) whereas the predominantly muddy fabrics require a low-energy setting below fair-weather wave-base. The relatively diverse macrobenthic fauna (mainly bivalves, some corals, calcareous sponges, gastropods, and echinoids) suggests fully marine conditions for the major part of the formation. However, the fauna tends to occur in beds and is not scattered throughout the otherwise fairly unfossiliferous succession, thus indicating potential fluctuations in environmental conditions maybe related to salinity changes (as indicated by repeated intercalation of evaporites). The predominance of fairly large epifaunal bivalves (pectinids such as *Radulopecten* and *Camptonectes*) suggest a relatively stable, oligotrophic environment (cf. Tomasovych 2006). The trace fossil assemblage is not very diagnostic and could be broadly assigned to the *Cruziana* ichnofacies (cf. Seilacher 1967). Typical elements of the nearshore *Skolithos* and the deeper shelf *Zoophycos* ichnofacies are missing. In summary, a lagoonal, mostly non-restricted environment for the Kamar-e-Mehdi Formation is inferred, representing the shelf-lagoon behind the barrier of the Esfandiar Platform. Water depth is inferred between a few meters (occasional oscillation ripples) to a few tens of meters at most (euphotic zone based on the presence of coral patch reefs). Jones and Desrochers (1992) suggested water depths of up to 30 m for shelf-lagoons of deeper warm-water rimmed shelves which are dominated by muddy sediments. The maximum depth of the lagoon behind the Great Barrier Reef of the Queensland shelf of NE Australia is 35 m (Hopley 1982). The modern Belize rimmed shelf has a lagoonal depth ranging from 6 to 60 m with an inshore siliciclastic facies (Ginsburg and James 1974; Jones and Desrochers 1992). However, water depth was certainly fluctuating and there is a general shallowing trend documented in the Kamar-e-Mehdi Formation (which is also seen in the section at Kuh-e-Bagh-e-Vang). The Echellon Limestone Member represents still relatively deep and open-marine conditions "inherited" from the underlying Baghamshah Formation, the middle part is predominantly fully marine, lagoonal, and the terminal Nar Limestone Member represents an increasingly restricted, peritidal environment capped by evaporites (Magu Gypsum Formation). Both the stratigraphic succession and facies development document the rise and demise of the Esfandiar Subgroup carbonate system: Early Callovian birth of the Esfandiar Platform following the uplift of the Shotori Swell (Fürsich et al. 2003b), barrier platform formation and expansion (Middle Callovian-Oxfordian; Fürsich et al. 2003a), and terminal tectonic disintegration related to the Late Cimmerian event (Wilmsen et al. 2003).

Relationship to the Esfandiar Platform

The section at Kuh-eh Bagh-e-Vang is intermediate between the Kamar-e-Mehdi and Esfandiar Limestone Formation and shows an interfingering of shelf-lagoon and platform facies (Fig. 13). Thus, the facies transition was more gradual without steep slope on the western side of the Esfandiar Platform, in contrast to its eastern side where gravitational deposits such as calcareous turbidites, mud- and debris flows as well as slumps and olistostromes have been recorded (Fürsich et al. 2003a). There was certainly a bathymetric difference between the platform close to sea level and the bottom of the lagoon, but not enough to lead to large-scale gravitational redeposition. The majority of the trough-crossbedded bio- and oolitic limestones represent shoal deposits. Their often poorly sorted and muddy internal fabric excludes, in our opinion, formation of these antiforms by constant wave energy of the open ocean (as in the case of the winnowed and well sorted marginal shoals at the eastern platform margin; Fürsich et al. 2003a, p. 182, pl. 34, Figs. 3–4). It is speculated here that these immature

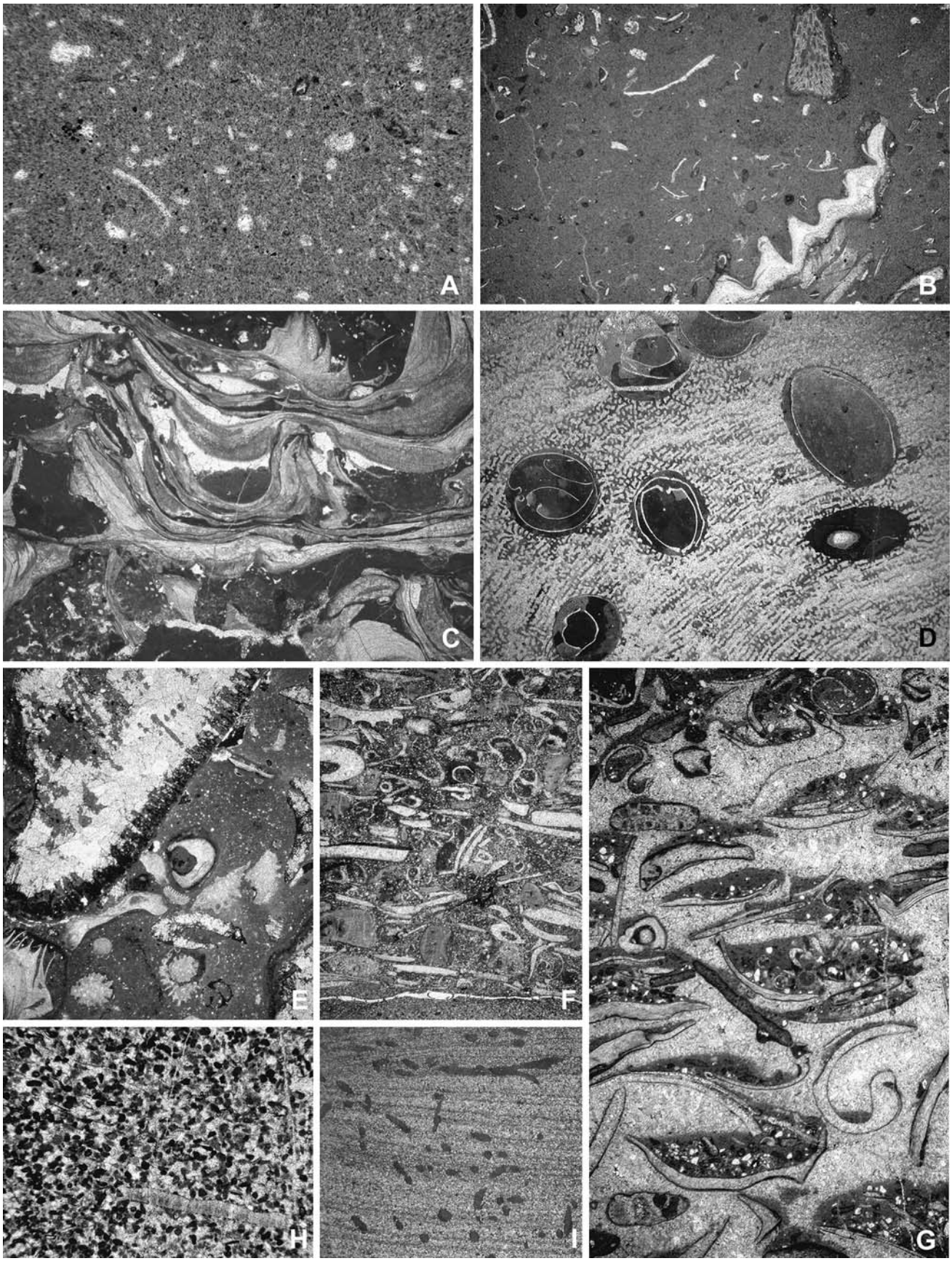

◀ **Fig. 9** Microfacies of the Kamar-e-Mehdi Formation. **a** Microbioclastic mud- to wackestone (FT 10). Road to Yazd section, sample 020218-6; width of photomicrograph is 2.5 mm. **b** Bioclastic wackestones (FT 11). Kalshaneh section, sample 010212-6; width of photomicrograph is 10 mm. **c** *Nanogyra* framestone (FT 12). Kuh-e-Bagh-e-Vang section, sample 010223-IR24; width of photomicrograph is 10 mm. **d** Microsolenid coral strongly bored by bivalves (coral framestone of FT 13). Note nestling bivalves in borings. Road to Yazd section, sample 020218-8; width of photomicrograph is 10 mm. **e** Bioclastic coral rudstone (FT 14) adjacent to coral patch reefs of facies type 13. Note taphonomic alteration of bioclasts. Road to Yazd section, sample 020218-2; width of photomicrograph is 7.5 mm. **f** Graded, sharp-based bioclastic packstone (FT 16a). Road to Yazd section, sample 020214-4; width of photomicrograph is 7.5 mm. **g** Graded bivalve rudstone of facies type 16b with sandfang in concave-up shells. Road to Yazd section, sample 020214-5; width of photomicrograph is 7.5 mm. **h** Well-sorted, intraclast grainstone with shell fragment (FT 17). Echellon section, sample 970224-2; width of photomicrograph is 2.5 mm. **i** Low-angle cross-bedded silt- to very fine grained sandstone with *Chondrites* isp. (FT 18). Road to Yazd section, sample W38-99; width of photomicrograph is 8 mm

shoals characterize the leeward margin of the Esfandiar Platform and most of the material was transported off the platform during storms (the same seems to be true for carbonate mud; see below). It may well be possible that the thick, trough-crossbedded units in this section are in fact clinoforms. The fact is, however, the Esfandiar Platform enlarged its platform interior and finally prograded on its debris westward into the lagoon (Figs. 7, 13). There are nine progradational–retrogradational cycles stacked onto each other in the section of Kuh-e-Bagh-e-Vang (Fig. 13) which reflect variations in accommodation space. They should correspond to the nine depositional sequences recognized by Fürsich et al. (2003a) from the eastern slope sections of the Esfandiar Platform within the Qal'eh Dokhtar Limestone Formation. However, it is impossible to recognize these cycles in the Kamar-e-Mehdi Formation.

An E–W transect (Fig. 13) from the Esfandiar Platform (section at Kuh-e-Gelkan; see Fürsich et al. 2003a for details) via Kuh-e-Bagh-e-Vang to the Echellon area shows the general increase in thickness towards the west (approximately doubling from the platform into the western shelf-lagoon). The section at Kuh-eh Bagh-e-Vang is intermediate in thickness and facies. This observation is consistent with the interpretation of the Esfandiar Platform sitting on the crest (Shotori Swell) of a west-vergent fault-block represented by the Tabas Block (Fürsich et al. 2003a). Constant and slow rotation of the Tabas Block around a horizontal N–S axis explains the differential subsidence and the observed facies zonation of the carbonate system of the Esfandiar Subgroup very well (Figs. 13, 14). This subsidence pattern characterized the entire (Middle) Callovian–Oxfordian interval and there is no evidence for a rapid tectonic pulse creating relief followed by subsequent sediment infilling.

This correlation also suggests that the bulk of the carbonate sediments produced by the Esfandiar Subgroup carbonate system was in fact deposited in the lagoon which provided enough accommodation space due to the higher subsidence rates (the slope sediments represented by the Qal'eh Dokhtar Limestone Formation are, compared to the Kamar-e-Mehdi Formation, spatially much more restricted and much thinner; Fig. 14 and Schairer et al. 2000; Fürsich et al. 2003a).

Accumulation rates and cyclicity

The Kamar-e-Mehdi Formation was deposited during the Callovian–Oxfordian, i.e., within ca. 9 myr according to Gradstein et al. (2004), and there are no indications of major stratigraphic gaps in the succession. A simple division of the maximum thickness (1,350 m) by this interval reveals sedimentation rates of 150 m/myr, which are normal for carbonate systems (Bosscher and Schlager 1993). However, the shelf-lagoonal accumulation rates are twice as high as those of the Esfandiar Platform (ca. 80 m/myr; Fürsich et al. 2003a). The mean accumulation rates of 150 m/myr and the mean thickness (3 m) of the ubiquitous lagoonal carbonate cycles of the Kamar-e-Mehdi Formation (Fig. 12) relate these high-frequency cycles to the ~20-kyr precession signal of the Milankovitch orbital frequencies. Thus, we speculate that the high-frequency carbonate cycles in fact represent precession cycles. The repetitive lithologies (cycles) and uniform depositional environment of the Kamar-e-Mehdi Formation suggest equilibrium conditions between sedimentation and accommodation space over a considerable period of time (Callovian–Oxfordian). This equilibrium phase was related to tectonic stability of the Tabas Block (cf. Seyed-Emami et al. 2004a) and a rising second-order eustatic sea level (e.g., Hallam 2001).

The Esfandiar Platform was in general a muddy system with high-energy sediments only occurring at the eastern rimmed margin (Fürsich et al. 2003a; Bagi and Tasli 2007). The large-scale platform interior was mud-dominated and obviously significant quantities of carbonate mud and peloids were exported into the shelf-lagoon as suspended material, episodically accompanied by skeletal grains and intraclasts in the form of tempestites. The cyclic sedimentation observed in the lagoon (high-frequency carbonate cycles) may be explained by variations in carbonate export related to the efficiency of the carbonate factory of the Esfandiar Platform: sedimentation rate was low in the bivalve shell beds (enrichment of hard parts, some encrusting, boring or abrasion) and followed by increasing export of mud and peloids throughout the cycles. Highstand shedding of the Esfandiar Platform during third-order depositional sequences

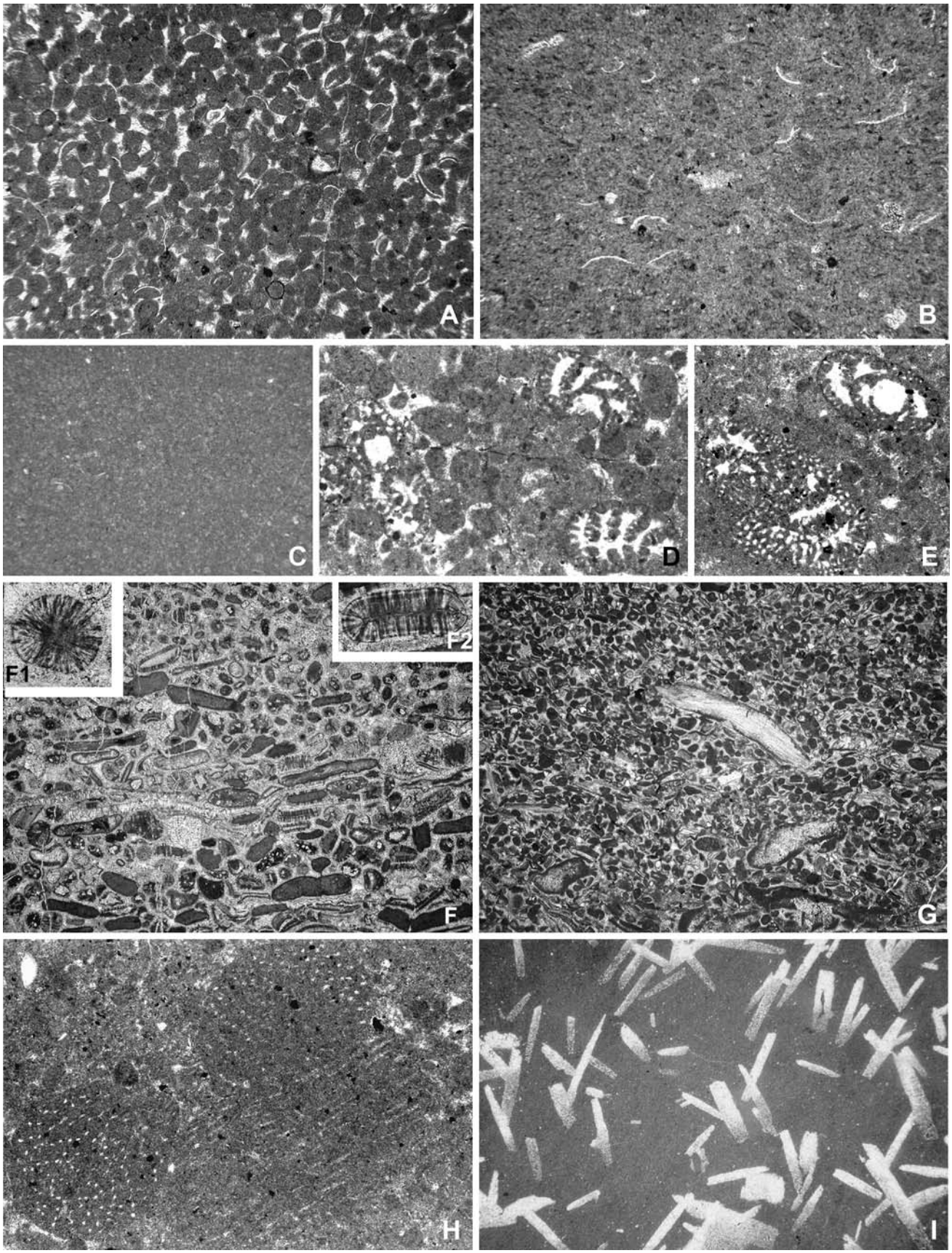

◀ **Fig. 10** Microfacies of the Nar Limestone Member of the Kamar-e-Mehdi Formation. **a** Well-sorted peloid grainstone (FT 23). Echellon section, sample 010214-2; width of photomicrograph is 2.5 mm. **b** Peloidal ostracod wackestone (FT 22). Echellon section, sample 010227-RI25; width of photomicrograph is 2.5 mm. **c** Mudstone (FT 20). Echellon section, sample 010227-RI21; width of photomicrograph is 2.5 mm. **d** Peloid pack- to grainstone (FT 23) with complex agglutinating foraminifera (*Alveosepta* sp.). Echellon section, sample 010214-3; width of photomicrograph is 2.5 mm. **e** Complex agglutinating foraminifera [*Alveosepta* cf. *personata* (Tobler), oblique section) within facies type 23. Echellon section, sample 010214-3; width of photomicrograph is 1.5 mm. **f** Graded bioclast-ooid grainstone (FT 25). Echellon section, sample 010227-RI23b; width of photomicrograph is 10 mm. **f1** Enlarged ooid of facies type 25; width of photomicrograph is 0.5 mm. **f2** Enlarged flattened ooid of facies type 25; width of photomicrograph is 0.7 mm. **g** Weakly graded, bioclastic intraclast grainstone (FT 26). Echellon section, sample 010227-RI23c; width of photomicrograph is 10 mm. **h** Crustacean coprolite packstone (FT 24). Echellon section, sample 010214-1; width of photomicrograph is 2.5 mm. **i** Mudstone with gypsum pseudomorphs (FT 21). Road to Yazd section, sample 990305-2; width of photomicrograph is 10 mm

was recorded by Fürsich et al. (2003a) in slope and basinal areas, but it obviously operated also on high-frequency (precession?) cycles due to periodic flooding and emergence of the platform interior feeding the lagoon (see Wilmsen and Neuweiler 2008, for a Liassic example). A significant amount of sediment was certainly also produced within the shelf-lagoon by the macrobenthic invertebrate communities. Surprisingly, there are so far no records of other typical lagoonal carbonate producers such as dasycladalean and udoteacean algae from the Kamar-e-Mehdi Formation (there are also only a few records of calcareous algae from the Esfandiar Platform; Fürsich et al. 2003a). Microbial whitings may have played an additional role for the lagoonal carbonate mud budget but the complex processes involved into their formations are not yet fully understood (Thompson et al. 1997; Thompson 2000).

Source of the siliciclastics

The source of the siliciclastic material within the Kamar-e-Mehdi Formation must have been the Yazd Block in the west because the siliciclastic content diminishes towards the east where the formation interfingers with the pure carbonates of the Esfandiar Limestone Formation. This scenario is comparable to the situation in the modern shelf-lagoon of the Belize rimmed shelf where the carbonate content of the lagoonal sediments changes from 30% nearshore to 90% near the barrier reef (Jones and Desrochers 1992). The occurrence of the Kamar-e-Mehdi Formation in typical fine-grained marl facies at Kalshaneh and west of Kamar-e-Mehdi (Figs. 1, 14) suggests that the Kalshaneh/Kalmard Fault was, at that time, not an important boundary between the Tabas and the (emergent) Yazd

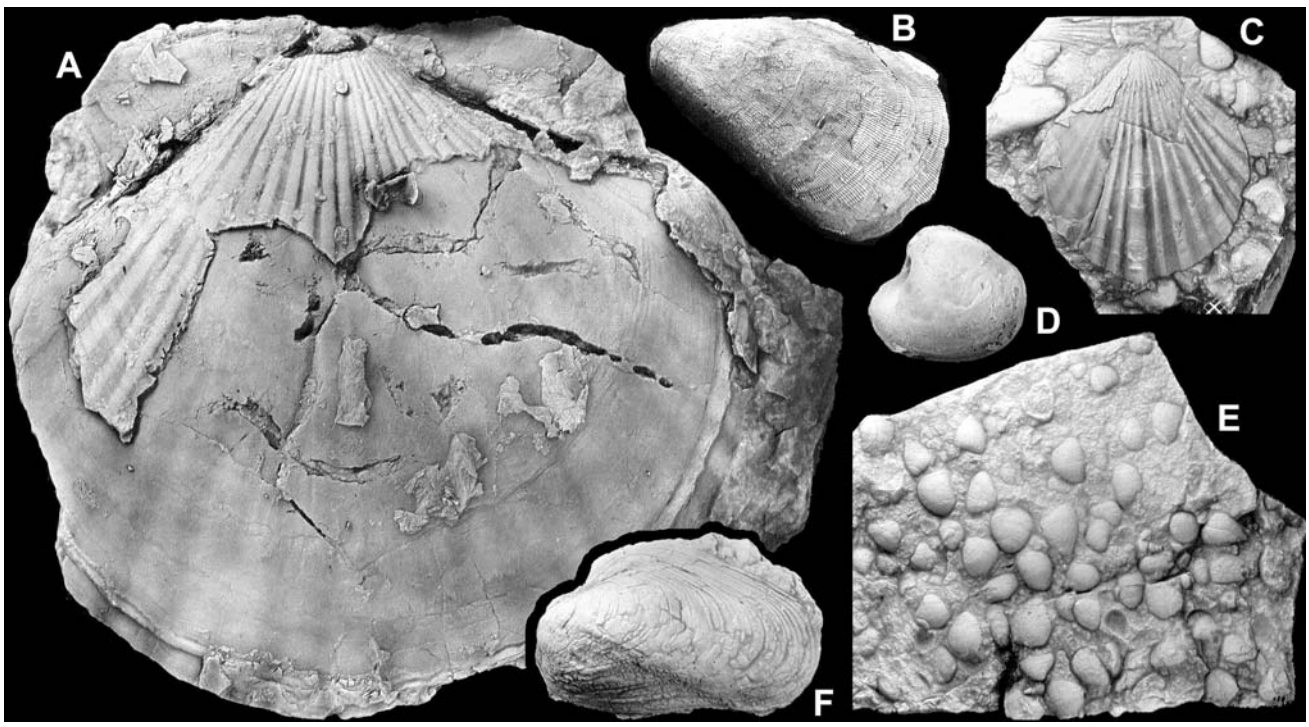

Fig. 11 Typical bivalves of the Kamar-e-Mehdi Formation (all figures in natural size). **a**, **c** *Radulopecten tipperi* (**a** = PIW2003IV-21; **c** = PIW2003IV-18). **b** *Arcomytilus pectinatus* (PIW2003IV-22). **d** *Ceratomya* sp. A (PIW2003IV-23). **e** Pavement of *Corbulomima* sp. (PIW2003IV-27). **f** *Modiolus bipartitus* (PIW2003IV-26)

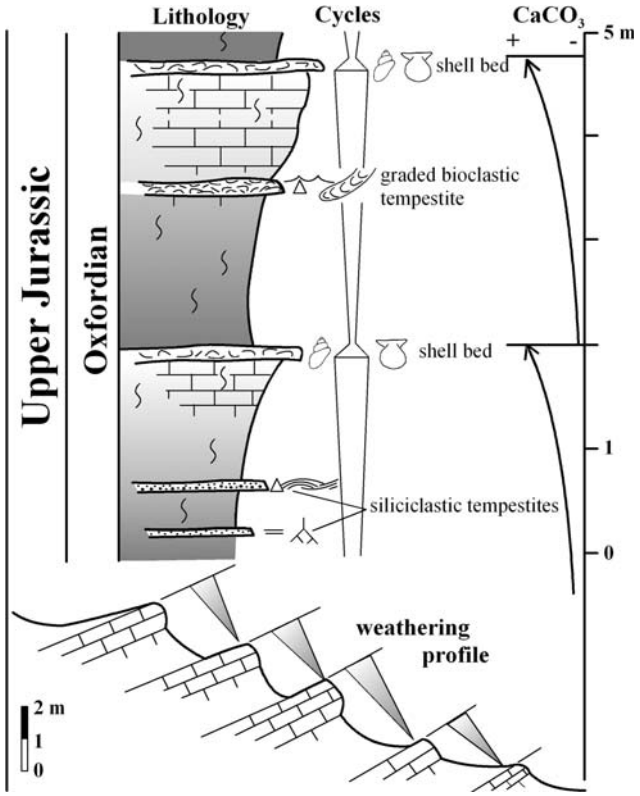

Fig. 12 Typical small-scale carbonate cycles (weathering profiles) from the Kamar-e-Mehdi Formation of the Echellon area (see Fig. 1 for location). For key of symbols see Fig. 7

Block where continental deposition prevailed (siliciclastic Chah Palang Formation of the Khur area; see Aistov et al. 1984; pers. obs.). The major block-bounding fault, therefore, was the Naini Fault further in the west (Fig. 14). Siliciclastic input was, however, limited (storm beds, aeolian dust?) which can be explained by the semi-arid to arid climate inhibiting significant fluvial input. Southwest of the Parvadeh mine (Aghanabati 1998: 517-518), in the south of the study area, coarse, partly conglomeratic sandstones occur at the base of the formation which further south, in the Cheghouki valley, thicken and turn reddish. Their deposition may be related to tectonic movements along the Naini Fault as time-equivalent, syntectonic sediments known as the Sikhor Formation were deposited along the Nayband Fault at the eastern margin of the Tabas Block (Fig. 14; Fürsich et al. 2003b).

Palaeogeographic and geodynamic synthesis

The Kamar-e-Mehdi Formation can be traced from Kalshaneh in the north of the Tabas Block to the south of the type area at around Kuh-e-Koleh-Nar (cf. Figs. 1, 14). This corresponds to a N–S distribution along strike of at least 150 km. In the E–W direction, the formation crops out in a 50 to 80-km-wide belt between the Yazd Block in the west and the platform facies of the Esfandiar Limestone Formation characterizing the eastern margin of the northern Tabas Block from Honu in the north to south of the type area at Kuh-e-Esfandiar (Fürsich et al. 2003a, 2003b; Figs. 1, 14). Together with the slope and basinal sediments of the Qal'eh Dokhtar and Korond Formations across the block-bounding Nayband Fault and onto the western Lut Block, the four formations of the Esfandiar Subgroup represent a large-scale carbonate system consisting of a shelf-lagoon, barrier platform and slope-to-basin area (Fig. 14). Temporal equivalents of the Kamar-e-Mehdi Formation are known as far as 500 km south of Tabas as the "Pectiniden-Gips-Fazies" from north of Kerman (Huckriede et al. 1962; Wilmsen et al. 2009a). Thus, the size of the Esfandiar Subgroup carbonate system (>500 km N–S, 50–100 km E–W) makes it an exceptional Mesozoic carbonate system, the dimensions of which approach those of the modern northeastern Australian Queensland Shelf with its about 10–50 km wide and less than 35 m deep lagoon and 1,500 km long and narrow (5–10 km) shelf-edge barrier reef (Hopley 1982).

The thick successions of gypsum-mudstone alternations within the upper Kamar-e-Mehdi Formation, including the terminal Nar Limestone Member with gypsiferous mudstones, indicate increasing restriction of the shelf-lagoon and net-evaporation. The increasing importance of evaporites towards the south indicates a main connection with the open ocean in the north ("Strait of Esfak"; see Fig. 14). According to Sarg (2001), an interfingering of carbonates and sulfates is, in general, interpreted to occur in a broad, shallow-marine hypersaline shelf-lagoon behind the main restricting shelf-edge carbonate complex (in this case represented by the Esfandiar Limestone Formation). Flooding of the shelf-lagoon resulted in widespread carbonate deposition dominated by skeletal-poor peloid mud- to wackestones (the majority of the Kamar-e-Mehdi Formation). Progressive restriction (due to net-evaporation or cut-off by the barrier platform processes) caused brining-upward and deposition of lagoonal gypsum related to highstand conditions of sea level. The Magu Gypsum Formation capping the Kamar-e-Mehdi Formation is, in this respect, interpreted as an "evaporate giant", marking the end of an arid basin-fill cycle (cf. Sarg 2001). Its deposition was related to a major evaporative drawdown of basin waters during the second-order sea-level lowstand associated with the Late Cimmerian tectonic event which can be traced all across the Iran Plate (Wilmsen et al. 2003, 2009a). The Magu Gypsum Formation may form an effective seal for hydrocarbon reservoirs in the east-central Iranian area.

The Esfandiar Subgroup is part of a belt of carbonate systems lining the margin of the Iran Plate during the Callovian and the Late Jurassic (Fig. 15). In the Alborz

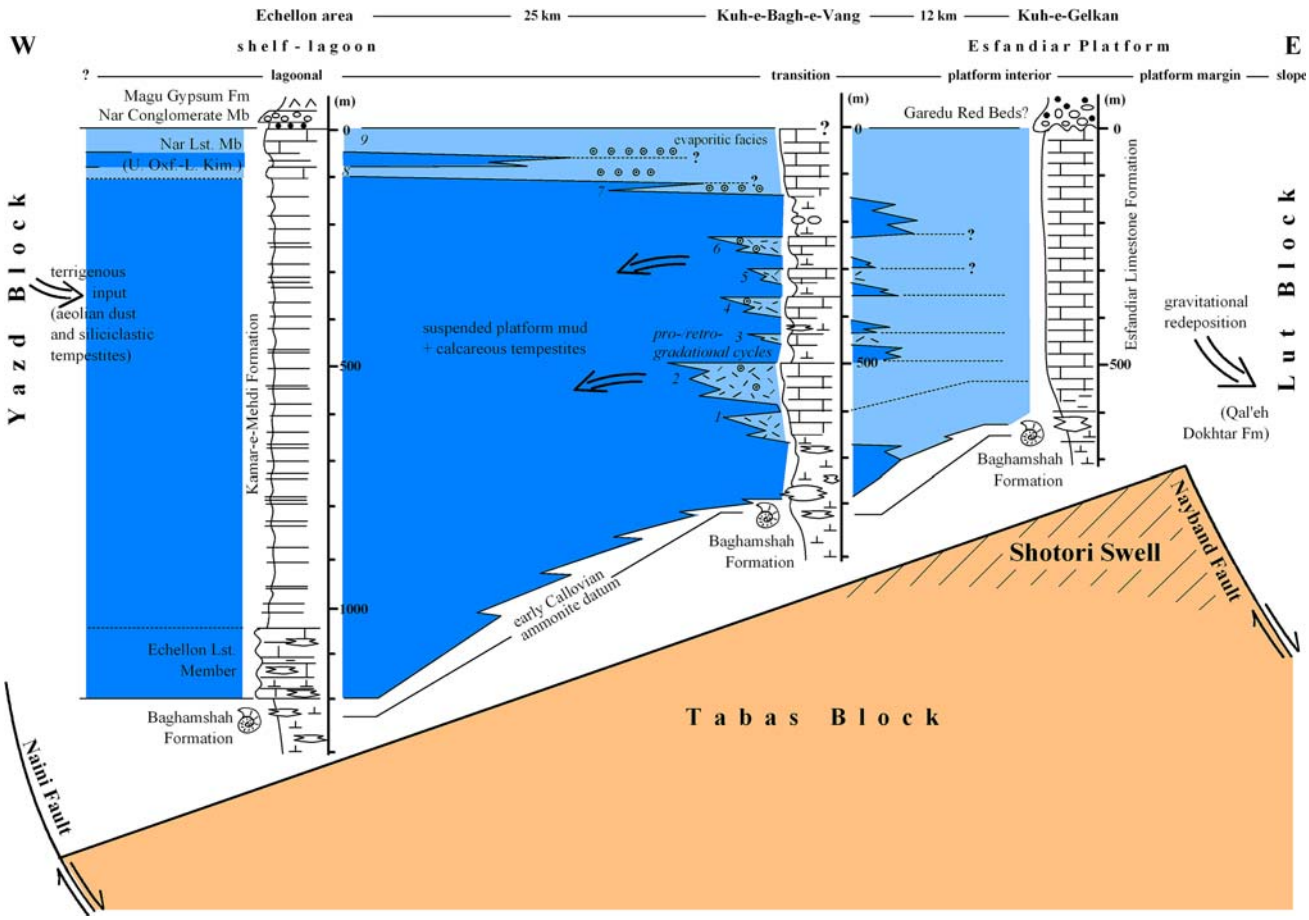

Fig. 13 E-W transect of the Callovian to Lower Kimmeridgian Esfandiar Subgroup from the platform (Esfandiar Limestone Formation on Shotori Swell) into the shelf-lagoon (Kamar-e-Mehdi Formation). Note the thickness increase from E to W and the interfingering of platform and shelf-lagoonal facies in the Kuh-e-Bagh-e-Vang section. *Numbers in italics* refer to pro-/retrogradational cycles discussed in the text

and Binalud Mountains of northern and northeastern Iran, this platform phase is represented by the carbonate system of the Dalichai and Lar Formations (e.g., Majidifard 2008). This large-scale carbonate system (>1,000 km W–E extension) traced the southern margin of the oceanic South Caspian Basin which rifted during Toarcian-Bajocian and potentially reached the spreading stage in the Bathonian-Late Jurassic (Brunet et al. 2003; Fürsich et al. 2005, 2009; Taheri et al. 2009). The limited siliciclastic input into these carbonate systems indicates a low relief of the emergent regions of the Iran Plate, its structural separation from Eurasia, and a (semi-)arid climate. The likewise large-scale carbonate system of the Mozduran Formation (Lasemi 1995) lined the northern (i.e., Turan Plate) margin of the eastern part of the South Caspian Basin in the present-day Koppeh Dagh Mountains (the Kashafrud Basin of Taheri et al. 2009; Fig. 15). The continuation from the Binalud Mountains of northeast Iran (where the Dalichai and Lar formations are well represented NW of Mashad) into the Esfandiar Subgroup of the Tabas Block is obscured by the absence of outcrops between the northernmost exposures of the latter north of Honu (Fig. 1) and post-Jurassic faulting and metamorphism related to marginal ocean basin development and closure around the Central-East Iranian Microcontinent (CEIM), starting in the Early Cretaceous (e.g., Lindenberg et al. 1983; Lindenberg and Jacobshagen 1983; Tirrul et al. 1983; Dercourt et al. 1986; Wilmsen et al. 2005). However, some kind of lateral continuation around the northeastern tip of the Iran Plate between the Lar and Esfandiar carbonate systems must have existed in order to explain their broadly similar facies pattern (cf. Fürsich et al. 2003a; Majidifard 2008). In Fig. 15, the three blocks of the CEIM are placed in a pre-rotational position, roughly parallel to the Neotethys subduction zone, with the Lut Block in a back-arc setting close to an inferred volcanic arc (cf. Wilmsen et al. 2009a). This interpretation is supported by the presence of volcanic rocks (pillow lavas, palagonitic tuffs, and keratophyre dykes) intercalated in a marine, shaly unit of Jurassic age

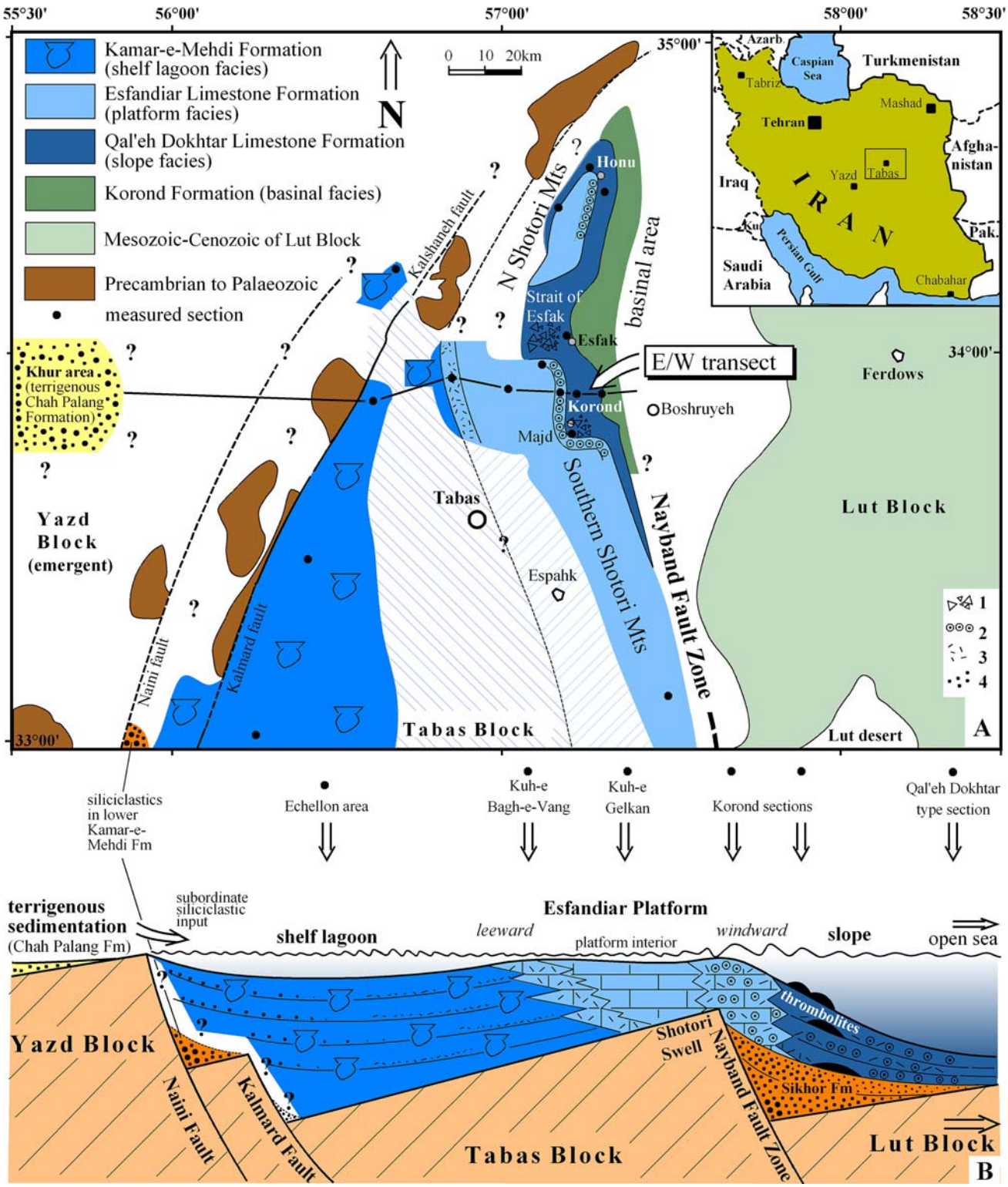

Fig. 14 Early-Middle Oxfordian palaeogeography of the northern Tabas Block (**a**) showing the distribution of the Esfandiar Subgroup carbonate system and (**b**) cross section inferred from E to W transect of measured sections as indicated in (**a**). Key: *1* slope magabreccia; *2* high-energy, oolitic platform margin shoals; *3* bioclastic shoals; *4* terrigenous sediments

(Stöcklin et al. 1972) and the Jurassic Shah-Kuh granite (Esmaeily et al. 2007) in the present-day eastern Lut Block, related to back-arc and arc magmatism associated with N-directed Neotethys subduction. The Esfandiar Subgroup thus represents a large-scale Neotethys Ocean-facing carbonate margin.

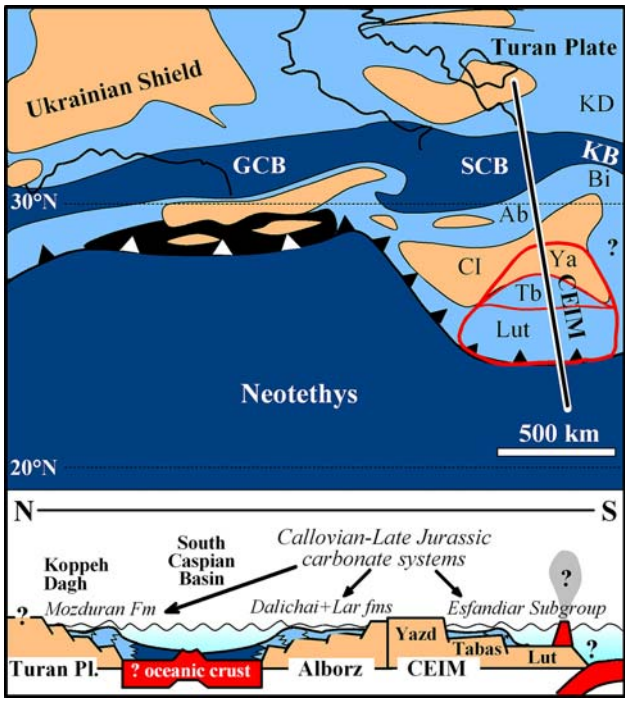

Fig. 15 Callovian—Late Jurassic carbonate systems of Iran (base map modified after Thierry 2000). The Lut, Tabas and Yazd Blocks are shown in assumed Jurassic orientation. *Ab* Alborz, *Bi* Binalud Mountains, *CI* Central Iran, *GCB* Greater Caucasus Basin, *KB* Kashafrud Basin, *KD* Koppeh Dagh, *SCB* South Caspian Basin

Conclusions

An integrated stratigraphic and facies analysis of the Callovian to Lower Kimmeridgian Kamar-e-Mehdi Formation of the Tabas Block of east-central Iran revealed the following results:

- The marly-calcareous Kamar-e-Mehdi Formation is up to 1,350 m thick and contains a basal Echellon Limestone Member (up to 180 m thick) and a terminal Nar Limestone Member (up to 100 m thick). The formation was deposited in a large-scale shelf-lagoon with a maximum water depth of up to a few tens of meters.
- The Echellon Limestone Member represents still relatively deep and open-marine conditions "inherited" from the underlying Baghamshah Formation, the middle part is lagoonal but predominantly fully marine, and the terminal Nar Limestone Member represents an increasingly restricted, peritidal environment capped by evaporites.
- The Kamar-e-Mehdi Formation is part of the large-scale carbonate system of the Esfandiar Subgroup, consisting of a shelf-edge carbonate platform (Esfandiar Limestone Formation) with an eastern slope and basinal area (Qal'eh Dokhtar Limestone and Korond Formations) and a western shelf-lagoon (Kamar-e-Mehdi Formation). This system can be traced N–S on the Tabas Block for about 500 km along strike and has a width of up to 100 km.
- An interfingering between the Kamar-e-Mehdi (shelf-lagoon facies) and Esfandiar Limestone Formation (platform facies) can be demonstrated. This observation supports the interpretation of the Esfandiar Platform sitting on the crest (Shotori Swell) of a west-vergent fault-block represented by the Tabas Block.
- The Kamar-e-Mehdi Formation was deposited within ca. 9 myr (Callovian–Oxfordian), suggesting sedimentation rates of 150 m/myr, twice as high as those of the Esfandiar Platform. The stratigraphic architecture of stacked meter-scale carbonate cycles and uniform environment of deposition of the Kamar-e-Mehdi Formation suggest equilibrium conditions between sedimentation and accommodation space, related to constant slow rotation of the Tabas Block around a horizontal axis.
- An important source for the lagoonal carbonate budget was the large-scale platform interior from which significant quantities of carbonate mud and peloids were exported into the shelf-lagoon as suspended material, episodically accompanied by skeletal grains and intraclasts in the form of tempestites. A significant amount of sediment was certainly also produced within the shelf-lagoon by the macrobenthic communities.
- The source of the siliciclastic material within the Kamar-e-Mehdi Formation must have been in the Yazd Block in the west because the siliciclastic content diminishes towards the east where the formation interfingers with the pure carbonates of the Esfandiar Limestone Formation.
- The relatively diverse macrobenthic fauna (mainly bivalves, some corals, calcareous sponges, gastropods, and echinoids) suggests normal marine conditions for the major part of the Kamar-e-Mehdi Formation. However, towards the upper part, increasing restriction caused biotic impoverishment and the deposition of skeletal-poor, evaporitic sediments.
- The Magu Gypsum Formation capping the Kamar-e-Mehdi Formation is an "evaporate giant", marking the end of an arid basin-fill cycle. The Magu Gypsum Formation may form an effective seal for hydrocarbon reservoirs in the east-central Iranian area.
- The Esfandiar Subgroup is part of a belt of carbonate systems tracking the margins of the Iran and Turan plates during the Callovian and the Late Jurassic (Dalichai and Lar formations of the Alborz and Binalud mountains, Mozduran Formation of the Koppeh Dagh). The Esfandiar Subgroup carbonate system represents a large-scale Neotethys-facing carbonate margin.

Acknowledgments This manuscript greatly benefited from insightful reviews by R. Henrich (Bremen, Germany) and M. Reolid (Jaén, Spain). Field work was financially supported by the National Geographic Society (grant # 5888-97) which we gratefully acknowledge. We also acknowledge logistic support by the University of Tehran, the Geological Survey of Iran (GSI), Tehran, and the Tabas Coal Company. M. Mehdi (Kénitra, Morocco) kindly determined the agglutinating foraminifera.

References

Aghanabati SA (1977) Etude géologique de la region de Kalmard (W. Tabas). Stratigraphie et tectonique. Geol Surv Iran Rep 35:230

Aghanabati SA (1998) Jurassic stratigraphy of Iran, Vol. 1 + 2. Geol Surv Iran, Tehran, p 746

Aistov L, Melnikov B, Krivyakin B, Morozov L, Kiristaev V (1984) Geology of the Khur area (central Iran). Explanatory text of the Khur quadrangle map 1:250.000. V/O Technoexport Rep 20:130

Bagheri S (2008) Anticlockwise rotation of the Central-East Iranian Microcontinent and the Eurasian–Indian collision. Intern Geol Congr Abstr Vol 33, abstr 1287304

Bagheri S, Stampfli GM (2008) The Anarak, Jandaq and Posht-e-Badam metamorphic complexes in central Iran: new geological data, relationships and tectonic implications. Tectonophysics 451:123–155. doi:10.1016/j.tecto.2007.11.047

Bagi H, Tasli K (2007) Paleoenvironmental analysis and biostratigraphy of the Upper Jurassic Esfandiar Formation (East-Central Iran). N Jb Geol Paläont 243:101–111

Bassoullet JP (1997) Les grands foraminifères. In: Cariou E, Hantzpergue P (eds) Biostratigraphie du Jurassique ouest-Européen et Méditerranéen. Mém Centres Rech Explo-Prod Elf Aquitaine 17:294–304

Bosscher H, Schlager W (1993) Accumulation rates of carbonate platforms. J Geol 101:345–355

Brunet M-F, Korotaev MV, Ershov AV, Nikishin AM (2003) The South Caspian Basin: a review of its evolution from subsidence modelling. Sediment Geol 156:119–148. doi:10.1016/S0037-0738(02)00285-3

Dercourt J, Zonenshain LP, Ricou L-E, Kazmin VG, Le Pichon X, Knipper AL, Grandjacquet C, Sbortshikov IM, Geyssant J, Lepvrier C, Pechersky DH, Boulin J, Sibuet J-C, Savostin LA, Sorokhtin O, Westphal M, Bazhenov ML, Lauer JP, Biju-Duval B (1986) Geological evolution of the Tethys belt from the Atlantic to the Pamir since the Lias. Tectonophysics 123:241–315. doi:10.1016/0040-1951(86)90199-X

Dunham RJ (1962) Classification of carbonate rocks according to depositional texture. In: Ham WE (ed) Classification of carbonate rocks. Am Assoc Petrol Geol Mem 1:108–121

Embry AF, Klovan JE (1972) Absolute water depth limits of Late Devonian paleoecological zones. Geol Rundsch 61:672–686. doi:10.1007/BF01896340

Enay R, Guiraud R, Ricou L-C, Mangold C, Thierry J, Cariou E, Bellion Y, Dercourt J (1993) Callovian (162 to 158 Ma). In: Dercourt J, Ricou LE, Vrielynck B (eds) Atlas Tethys palaeoenvironmental maps. Gauthier-Villars, Paris, pp 81–95

Esmaeily D, Bouchez JL, Siqueira R (2007) Magnetic fabrics and microstructures of the Jurassic Shah-Kuh granite pluton (Lut Block, Eastern Iran) and geodynamic inference. Tectonophysics 439:149–170. doi:10.1016/j.tecto.2007.04.002

Fürsich FT, Wilmsen M, Seyed-Emami K, Schairer G, Majidifard MR (2003a) Platform/basin transect of a large-scale Middle-Late Jurassic carbonate platform system (Shotori Mountains, Tabas area, east-central Iran). Facies 48:171–198. doi:10.1007/BF02667538

Fürsich FT, Wilmsen M, Seyed-Emami K, Majidifard MR (2003b) Evidence of synsedimentary tectonics in the northern Tabas Block, east-central Iran: the Callovian (Middle Jurassic) Sikhor Formation. Facies 48:151–170. doi:10.1007/BF02667537

Fürsich FT, Wilmsen M, Seyed-Emami K, Cecca F, Majidifard MR (2005) The upper Shemshak Formation (Toarcian-Aalenian) of the Eastern Alborz (Iran): biota and palaeoenvironments during a transgressive–regressive cycle. Facies 51:365–384. doi:10.1007/s10347-005-0051-z

Fürsich FT, Wilmsen M, Seyed-Emami K, Majidifard MR (2009) The Mid-Cimmerian tectonic event (Bajocian) in the Alborz Mountains, northern Iran: evidence of the break-up unconformity of the South Caspian Basin. In: Brunet M-F, Wilmsen M, Granath J (eds) South Caspian to Central Iran basins. Geol Soc Lond Spec Publ 312:189–203

Ginsburg RN, James NP (1974) Holocene carbonate sediments of continental margins. In: Burke CA, Drake CL (eds) The geology of continental margins. Springer, Berlin Heidelberg New York, pp 137–155

Gradstein FM, Ogg JG, Smith AG (2004) A geologic time scale 2004. University Press, Cambridge, p 589

Hallam A (2001) A review of the broad pattern of Jurassic sea-level changes and their possible causes in the light of current knowledge. Palaeogeogr Palaeoclimatol Palaeoecol 167:23–37. doi:10.1016/S0031-0182(00)00229-7

Hopley D (1982) The geomorphology of the Great Barrier Reef. Wiley, New York, p 453

Hottinger L (1967) Foraminifères imperforés du Mésozoïque marocain. Notes Mem Serv Geol Maroc 209:1–168

Huckriede R, Kürsten M, Venzlaff H (1962) Zur Geologie des Gebietes zwischen Kerman und Sagand (Iran). Beih Geol Jb 51:1–197

Jones B, Desrochers A (1992) Shallow platform carbonates. In: Walker RG, James NP (eds) Facies models: response to sea level change. Geol Assoc Canada, St. John's, pp 277–301

Lasemi Y (1995) Platform carbonates of the Upper Jurassic Mozduran Formation in the Kopet Dagh Basin, NE Iran–facies, palaeoenvironments and sequences. Sediment Geol 99:151–164. doi:10.1016/0037-0738(95)00041-6

Lindenberg HG, Jacobshagen V (1983) Post-Paleozoic geology of the Taknar Zone and adjacent areas (NE Iran, Khorasan). Geol Surv Iran Rep 51:145–163

Lindenberg HG, Görler K, Ibbeken H (1983) Stratigraphy, structure and orogenetic evolution of the Sabzevar Zone in the area of Oryan Khorasan, NE Iran. Geol Surv Iran Rep 51:120–143

Majidifard MR (2008) Stratigraphy and facies analysis of the Dalichai and Lar Formations (Middle-Upper Jurassic) of NNE Iran. Beringeria 39:3–49

Pandey DK, Fürsich FT (2003) Jurassic corals of east-central Iran. Beringeria 32:1–138

Ruttner A, Nabavi M, Hadjian J (1968) Geology of the Shirghest area (Tabas area, east Iran). Geol Surv Iran Rep 4:1–133

Sarg JF (2001) The sequence stratigraphy, sedimentology, and economic importance of evaporite-carbonate transitions: a review. Sediment Geol 140:9–42. doi:10.1016/S0037-0738(00)00170-6

Schairer G, Seyed-Emami K, Fürsich FT, Senowbari-Daryan B, Aghanabati SA, Majidifard MR (2000) Stratigraphy, facies analysis and ammonite fauna of the Qal'eh Dokhtar Formation at the type locality west of Boshrouyeh (east-central Iran). N Jb Geol Paläont Abh 216:35–66

Schairer G, Fürsich FT, Wilmsen M, Seyed-Emami K, Majidifard MR (2003) Stratigraphy and ammonite fauna of Upper Jurassic basinal sediments at the eastern margin of the Tabas Block (east-central Iran). Geobios 36:195–222. doi:10.1016/S0016-6995(03)00006-8

Sdzuy K, Monninger W (1985) Neue Modelle des "Jakobstabes". N Jb Geol Paläont Mh 1985:300–320

Seilacher A (1967) Bathymetry of trace fossils. Mar Geol 5:413–428. doi:10.1016/0025-3227(67)90051-5

Sengör AMC (1990) A new model for the late Palaeozoic-Mesozoic tectonic evolution of Iran and its implications for Oman. In:

Robertson AHF, Searle MP, Ries AC (eds) The geology and tectonics of the Oman region. Geol Soc Lond Spec Publ 49:797–831

Sengör AMC, Altiner D, Cin A, Ustaömer T, Hsü KJ (1988) Origin and assembly of the Tethysides orogenic collage at the expense of Gondwana Land. In: Audley-Charles MG, Hallam A (eds) Gondwana and Tethys. Geol Soc Lond Spec Publ 37:119–181

Seyed-Emami K, Alavi-Naini M (1990) Bajocian stage in Iran. Mem Descriz Carta Geol Ital 40:215–222

Seyed-Emami K, Schairer G, Aghanabati SA, Fazl M (1991) Ammoniten aus dem Bathon von Zentraliran (Tabas-Nayband Region). Münch Geowiss Abh A19:65–100

Seyed-Emami K, Schairer G, Aghanabati SA (1997) Ammoniten aus der Baghamshah Formation (Callov, Mittlerer Jura), NW Tabas (Zentraliran). Mitt Bay Staatsslg Paläont Hist Geol 37:24–40

Seyed-Emami K, Schairer G, Aghanabati SA, Fürsich FT, Senowbari-Daryan B, Majidifard MR (1998) *Cadomites* aus der unteren Baghamshah-Formation (Oberbathon, Mittlerer Jura) SW Tabas (Zentraliran). Mitt Bay Staatsslg Paläont Hist Geol 38:111–119

Seyed-Emami K, Fürsich FT, Schairer G (2001) Lithostratigraphy, ammonite faunas and palaeoenvironments of Middle Jurassic strata in North and Central Iran. Newsl Stratigr 38:163–184

Seyed-Emami K, Schairer G, Fürsich FT, Wilmsen M, Majidifard MR (2002) Reineckeiidae (Ammonoidea) from the Callovian (Middle Jurassic) of the Shotori Range (east central Iran). N Jb Geol Paläont Mh 2002:184–192

Seyed-Emami K, Fürsich FT, Wilmsen M (2004a) Documentation and significance of tectonic events in the northern Tabas Block (east-central Iran) during the Middle and Late Jurassic. Riv Ital Paleont Stratigr 110:163–171

Seyed-Emami K, Fürsich FT, Wilmsen M, Schairer G, Majidifard MR (2004b) Jurassic (Toarcian to Bajocian) ammonites from the Lut Block, east-central Iran. Acta Geol Polon 54:77–94

Soffel H, Davoudzadeh M, Rolf C, Schmidt S (1996) New palaeomagnetic data from Central Iran and a Triassic palaeoreconstruction. Geol Rundsch 85:293–302. doi:10.1007/BF02422235

Stampfli GM, Borel GD (2002) A plate tectonic model for the Paleozoic and Mesozoic constrained by dynamic plate boundaries and restored synthetic oceanic isochrones. Earth Planet Sci Lett 196:17–33. doi:10.1016/S0012-821X(01)00588-X

Stöcklin J, Eftekhar-Nezhad J, Hushmand-Zadeh A (1965) Geology of the Shotori Range (Tabas area, East Iran). Geol Surv Iran Rep 3:1–69

Stöcklin J, Eftekhar-Nezhad J, Hushmand-Zadeh A (1972) Central Lut reconnaissance, East Iran. Geol Surv Iran Rep 22:1–62

Taheri J, Fürsich FT, Wilmsen M (2009) Stratigraphy, depositional environments, and geodynamic significance of the Upper Bajocian-Bathonian Kashafrud Formation (NE Iran). In: Brunet M-F, Wilmsen M, Granath J (eds) South Caspian to Central Iran basins. Geol Soc Lond Spec Publ 312:205–218

Thierry J (2000) Middle Callovian (157–155 Ma). In: Dercourt J, Gaetani M, Vrielynck B, Barrier E, Biju-Duval B, Brunet M-F, Cadet JP, Crasquin S, Sandulescu M (eds) Atlas Peri-Tethys palaeogeographical maps. CCGM/CGMW, Paris, pp 71–97

Thompson JB (2000) Microbial whitings. In: Riding RE, Awramik SM (eds) Microbial sediments. Springer, Berlin Heidelberg New York, pp 250–260

Thompson JB, Schultze-Lam S, Beverige TJ, Marais DJD (1997) Whiting events: biogenic origin due to the photosynthetic activity of cyanobacterial picoplankton. Limnol Oceanogr 42:133–141

Tirrul R, Bell IR, Griffis RJ, Camp VE (1983) The Sistan suture zone of eastern Iran. Geol Soc Am Bull 94:134–150. doi:10.1130/0016-7606(1983)94<134:TSSZOE>2.0.CO;2

Tomasovych A (2006) Differential effects of environmental factors on the ecology of brachiopods and bivalves during the Late Triassic and Jurassic. PhD Thesis, Würzburg Univ, pp 430 [http://opus.bibliothek.uni-wuerzburg.de/volltexte/2006/1913/]

Wilmsen M, Neuweiler F (2008) Biosedimentology of the Early Jurassic post-extinction carbonate depositional system, central High Atlas rift basin, Morocco. Sedimentology 55:773–807. doi:10.1111/j.1365-3091.2007.00921.x

Wilmsen M, Fürsich FT, Seyed-Emami K (2003) Revised lithostratigraphy of the Middle and Upper Jurassic Magu Group of the northern Tabas Block, east-central Iran. Newsl Stratigr 39:143–156

Wilmsen M, Wiese F, Seyed-Emami K, Fürsich FT (2005) First record and significance of Cretaceous (Turonian) ammonites from the Shotori Mountains, east-central Iran. Cretac Res 26:181–195. doi:10.1016/j.cretres.2004.10.004

Wilmsen M, Fürsich FT, Seyed-Emami K, Majidifard MR (2009a) An overview of the lithostratigraphy and facies development of the Jurassic System on the Tabas Block, east-central Iran. In: Brunet M-F, Wilmsen M, Granath J (eds) South Caspian to Central Iran basins. Geol Soc Lond Spec Publ 312:323–344

Wilmsen M, Fürsich FT, Seyed-Emami K, Majidifard MR, Taheri J (2009b) The Cimmerian orogeny in northern Iran: tectono-stratigraphic evidence from the foreland. Terra Nova 21 (in press)